

## In Search of Lonely Top Quarks at the Tevatron

Matthew T. Bowen, Stephen D. Ellis, and Matthew J. Strassler

*Department of Physics, P.O. Box 351560, University of Washington, Seattle, WA 98195*

Single top-quark production, via weak-interaction processes, is an important test of the standard model, potentially sensitive to new physics. However, it is becoming known that this measurement is much more challenging at the Tevatron than originally expected. We reexamine this process and suggest new methods, using shape variables, that can supplement the methods that have been discussed previously. In particular, by focusing on correlations and asymmetries, we can reduce backgrounds substantially without low acceptance for the signal. Our method also allows for a self-consistency check on the modeling of the backgrounds. However, at the present time, serious systematic problems remain, especially concerning the background from  $W$ -plus-jets; these must be studied further by experimentalists and theorists alike.

PACS numbers: 14.65.Ha, 13.85.Ni, 13.85.Qk, 13.87.Ce

## I. INTRODUCTION

The electroweak production of single top quarks is an important standard model process which the Tevatron is guaranteed to be able to study. This reaction, which has been investigated previously [1, 2], is interesting both because it provides a direct measurement of the  $V_{tb}$  CKM element and because it is sensitive to deviations of top quark physics from standard model predictions, in particular, through their effects on the top-bottom- $W$  vertex [3]. Limits on single top production from Run I at the Tevatron have been published [4, 5], and the first Run II limits have appeared [6, 7]. In this article we discuss methods which we hope will improve the significance of the measurement by using more information encoded in the shape of the signal, in a way that will be less sensitive to systematic errors than a simple counting experiment. However, we also show that the size of the  $W$ -plus-jets background, and the difficulty of predicting it accurately, represent a serious obstacle.

Single top production is a very unusual process. At Fermilab energies, the “ $tb$ ” production of a top quark and bottom antiquark by an  $s$ -channel  $W$  boson, as can occur through the diagram in Fig. 1a, has a lower cross-section

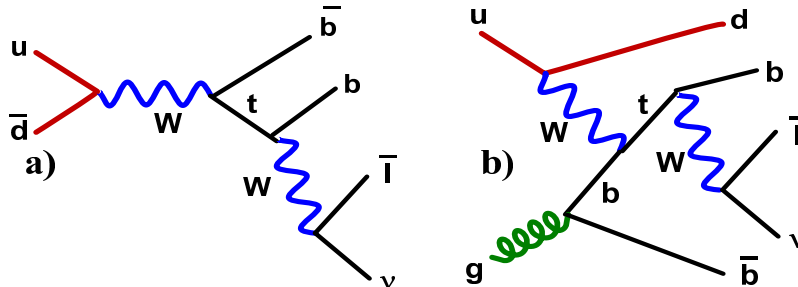


FIG. 1: Single top quark production via (a) an  $s$ -channel  $W$  boson; (b) a  $t$ -channel  $W$  boson.

than “ $tbq$ ”  $t$ -channel  $W$  boson of a  $t$ ,  $\bar{b}$ , and an extra light-quark jet near the beam axis, as occurs through diagrams such as that in Fig. 1b.<sup>1</sup> The  $tbq$  process has a distinct shape, both because of its unusual initial state, the hard light-quark jet (which has large  $p_T$  and large pseudo-rapidity) in the final state, and correlations between this jet and the lepton from the top decay. In this paper, we will explore a method for using these features to help separate single top from its major backgrounds:  $t\bar{t}$ ,  $W$  plus jets, and QCD events.

This separation using the shape of the event is essential, because a simple counting experiment is extremely difficult to carry out. Both our studies and recent data indicate that the size of the relevant  $W$ -plus-jets background is larger than anticipated a few years ago.[1, 2] This is compounded by other issues, such as the 2% decrease in Fermilab’s energy compared to expectations, and lower cross-section calculations for the signal [8, 9, 10]. We are concerned that systematic errors in the understanding of the background will plague a direct counting experiment at a level that will make any claims of discovery suspect. Thus, in our view, additional methods, independent of (but perhaps to be used in conjunction with) a counting experiment, are needed even for a discovery of the process, as well as for a precision measurement. We will argue that it is necessary, and possible, to reduce backgrounds further by using more information about the final states. (Note that a shape fit using a single variable was used in [4, 6].)

However, even with these improvements, our results suggest that the measurement of single top remains challenging. We have found that there is no simple way, even with  $3 \text{ fb}^{-1}$  of integrated luminosity, to achieve both good statistics and a satisfactory signal-to-background ratio. The essential problem, compared to earlier and more optimistic studies [1], is that the  $W$ -plus-jets sample with a single  $b$ -tagged jet is larger, less predictable, and more variegated than was understood a few years ago. We will discuss in some detail the difficulties with this background, and the need for a wide range of efforts to bring it under control.

The organization of this paper is as follows. In Section II we discuss the general structure of the events expected for both signal and background events. Section III includes a detailed discussion of how we have simulated both types of events, the cuts used to define the event samples, the expected (and observed) differences between signal and background event shapes, and new observables intended to highlight these differences. In Section IV we address the essential issues of uncertainties, both statistical and systematic, with a special focus on the difficulties inherent

<sup>1</sup> There is, as always, some ambiguity as to whether the initial state contains a gluon which splits into a  $b$  and  $\bar{b}$  as part of the scattering process or whether the initial state contains a  $b$  parton directly, *i.e.*, the splitting process is part of the incoming wave function. Since the  $\bar{b}$  jet is generally not used in the analysis below, a careful examination of this separation is not essential for us.

in understanding the background arising from  $W$  boson production accompanied by jets. In the final section we summarize our analysis and our conclusions.

## II. THE BACKGROUNDS TO SINGLE TOP PRODUCTION

From Fig. 1b one can see that a  $tbq$  event has a final partonic state consisting of at least the following: a charged lepton, a neutrino,  $b$  and  $\bar{b}$  quarks, and a light quark. The bottom quark that comes directly from the initial gluon tends to have small transverse momentum, and is rarely in the pseudo-rapidity and  $p_T$  range necessary to be identified by  $b$ -tagging algorithms. Thus, in selecting  $t$ -channel signal events, one asks for (a) one or more  $b$ -tagged jets, (b) significant missing energy (from the neutrino), (c) one and only one isolated  $e^\pm$  or  $\mu^\pm$ , (d) at least one untagged jet. Typically, the highest- $p_T$  untagged jet in a  $t$ -channel event is that from the light quark. Also, in typical events a  $t$  quark can be reconstructed from the tagged jet and a  $W$ , itself reconstructed from the charged lepton and the missing energy. The kinematics of the event tend to prefer a total visible scalar-summed transverse energy of order  $m_t$ .

The  $tb$  process has a  $b$  quark jet and a  $\bar{b}$  jet, along with a lepton and a neutrino. In a significant number of events, one of the two  $b$ -jets will not be tagged, so that the same criteria used for  $tbq$  — one  $b$ -tagged jet, missing energy, a charged lepton and an untagged jet — will have moderately high efficiency for this process as well. Since the  $tb$  process is smaller in cross-section and considerably less distinctive in shape than  $tbq$ , and therefore harder to separate from background, it makes sense for us to optimize our approach for  $tbq$ . We will not, in this paper, discuss the measurement of the  $tb$  and  $tbq$  channels separately, as this will only be possible well after the initial measurements of the combined production process.

The main backgrounds to single top production, which all can imitate the signature just described, are [1] (1) “ $t\bar{t}$ ”, top quark pair production, primarily from events where only one of the top quarks decays leptonically, but also from events with two leptonic decays; (2) “QCD” events with fake missing energy and with either a fake lepton or a lepton from a heavy flavor decay; and, most problematic, (3) “ $Wj^n$ ” events with a leptonically-decaying  $W$  plus some number  $n \geq 2$  of quark or gluon jets.

### A. Top pair production

Top quark pair production is a formidable background to all single top channels. After both top quarks decay, there are two high- $p_T$   $b$  quarks, which typically give rise to at least one  $b$ -tagged jet, and two  $W$  bosons which can decay hadronically or leptonically. The signature for single top will be mimicked if only one  $W$  decays leptonically, or if both do and only one charged lepton is detected. The present measurement of the cross-section for  $t\bar{t}$  production has a large uncertainty, though this uncertainty is expected to drop to around 10% [11] by the end of Run II. However, even this systematic uncertainty would prohibit observation of single top above the  $t\bar{t}$  background, so a substantial amount of  $t\bar{t}$  must be cut away. The contribution of  $t\bar{t}$  with one hadronically decaying top is especially problematic, since often the leptonically-decaying top quark can be reconstructed. On the other hand, this background can be reduced using the fact that these events tend to exhibit considerably more transverse energy than true single top events, to have more jets, and to be more spherical. These kinematic handles are not present for events where both top quarks decay leptonically, but such events are suppressed by both the leptonic decay branching fraction and our requirement that only one  $e^\pm$  or  $\mu^\pm$  be observed in the detector. Furthermore, the accurate reconstruction of a leptonically-decaying top quark is more difficult in such events.

### B. QCD backgrounds

Pure QCD events can give rise to fake leptons and provide heavy-flavor jets (or jets which have no heavy-flavor but are mistagged.) As fluctuations in energy measurement can lead to a fake missing  $E_T$  signal, these QCD events form a background to single top production. While the energetics tend to be lower than in signal events, and the invariant mass of the “lepton”, missing energy and  $b$ -tagged jet exhibits no peak at  $m_t$ , the number of events is so large that it is not obvious, without data (or a complete detector simulation), whether this represents a relevant background. Recent results from DZero [7] indicate that the number of QCD events entering their single-top samples (defined by somewhat different cuts than used here) is smaller than for other backgrounds, and is, in first approximation, comparable in size to the single-top signal. This conclusion depends in detail on cuts and on the flavor of the lepton (muons being more prevalent than electrons in their samples) and may differ for CDF. As we will see, the methods that we describe below provide substantial further reduction of this QCD background and the systematic errors associated with determining

it, to the point that it should not pose a serious issue. Consequently, we will largely disregard the QCD contribution to the sample, except for a discussion in Sec. III.D as to when and why this is justified.

### C. $W$ plus jets

The  $W$ -plus-jets background is much more challenging. The  $Wj^n$  events potentially entering the sample consist of a real  $W$  boson decaying leptonically, and at least two other quarks or gluons in the final state. While the  $Wj^n$  events do tend to have smaller energetics than single top, and do not have a reconstructible  $t$  quark, the number of events is so large, and the energy resolution at Fermilab is sufficiently broad, that the  $Wj^n$  events form a large and problematic background to single-top production.

The difficulties involved in simulating  $Wj^n$  events have been discussed elsewhere [12, 13] and we will not give a full review, but it is important to note that there are special problems for the sample with a single  $b$ -tag that neither untagged nor double-tagged samples suffer from. In particular, many different partonic processes, with different shapes, contribute to the sample in a fashion which is difficult to predict accurately. We will discuss this in detail in section IV.D. As we will see, reducing the systematic error on the prediction and/or measurement of this process is essential for success.

## III. SIMULATIONS, CUTS, SHAPES AND METHODS

### A. Simulation and Kinematic Cuts

To model both signal and background, we have used MadEvent [14] to generate events, Pythia [15] to then simulate showering and hadronization (using the default value of the initial shower scale,  $\sqrt{\hat{s}}$ ), and PGS [16] to act as a fast detector simulation. The single top  $s$ - and  $t$ -channel cross-sections have been normalized to 0.88 pb and 1.98 pb respectively [8], and generated with factorization and renormalization scales  $\mu = m_t = 175$  GeV. For the  $t\bar{t}$  process, the cross-section is normalized to 6.7 pb [17] and generated with factorization and renormalization scales also at  $\mu = m_t = 175$  GeV. For the  $Wj^n$  channel, we have limited our simulations to  $W$ -plus-two-jets (henceforth  $Wjj$ ) at the MadEvent level, since we believe the uncertainties in our simulations of this process are as large as the contribution at the next order in  $\alpha_s$ . Samples for the  $Wjj$  channel were generated using a renormalization and factorization scale  $\mu = M_W/2$ , which is selected to give the correct normalization at next-to-leading order [18]. We employ cuts at the MadEvent level of  $p_{Tj_1}, p_{Tj_2} > 10$  GeV (where  $p_{Tj_i}$  is the transverse momentum of the  $i^{th}$  jet), with angular separation  $\Delta R(j_1, j_2) > 0.4$ , and  $|\eta_j| < 4.0$ .

The  $b$ -tagging is simulated as follows. Jets containing a  $b$  quark (either perturbatively or produced during showering) are taken to be tagged with an efficiency of the form  $0.5 \tanh(p_T/36 \text{ GeV})$ , where  $p_T$  is the transverse momentum of the jet. Jets containing a  $c$  quark (either perturbatively or produced during showering) are taken to be tagged with a rate of the form  $0.15 \tanh(p_T/42 \text{ GeV})$ , while jets containing no heavy flavor are taken to be mistagged with a rate of the form  $0.01 \tanh(p_T/80 \text{ GeV})$ .<sup>2</sup>

From the events generated in this fashion, we define our initial event sample to be those events that contain *one and only one* isolated charged lepton, missing energy, *one or more*  $b$ -tagged jets, and *one or more* untagged jets. These objects satisfy the “basic” cuts listed in Table I. The  $p_T$  constraints in this and later tables apply only to the highest- $p_T$   $b$ -tagged jet and the highest- $p_T$  untagged jet. Additional cuts are necessary in order to bring backgrounds down to a reasonable level.

Given that  $Wj^n$  tends, compared to the signal, to have lower energy and fewer jets, and that  $t\bar{t}$  tends to have higher energy and more jets, there are two natural choices of variables to cut on that take advantage of the overall kinematics of the events without appealing to event shapes. One possibility is to cut on the total transverse energy of the event; a second would be to cut on the number of high- $p_T$  jets. The question of which of these (or whether a

---

<sup>2</sup> There is no agreed-upon convention for the light-quark/gluon mistagging function. The tanh form of the mistagging function is *not* what is used in the default PGS detector simulation, which instead is  $-5.54 \times 10^{-5} + 1.66 \times 10^{-7}(p_T/1 \text{ GeV})^{2.507}$ . Based on the fact that this function leads to large mistagging rates at very high  $p_T$ , in contradiction to measurements at CDF [19], we have changed this mistagging function within PGS to a tanh form. The overall mistagging rate that we use is larger than assumed in other papers, including [1] and the recent work of [9], where the size of  $Wj^n$  backgrounds is smaller as a result. The true form of the mistagging function is detector- and algorithm-dependent, and different mistagging functions do change the shape of certain distributions. Our results suggest that uncertainties in this function lead to important, but not dominant, systematic uncertainties in the  $Wj^n$  background.

Item	$p_T$	$ \eta $
$\ell^\pm$	$\geq 15$ GeV	$\leq 2$
MET ( $\nu$ )	$\geq 15$ GeV	-
jet ( $b$ -tag)	$\geq 20$ GeV	$\leq 2$
jet (no $b$ -tag)	$\geq 20$ GeV	$\leq 3.5$

TABLE I: Basic cuts for initial sample. Here  $p_T$  is the transverse momentum and  $\eta$  is the pseudo-rapidity.

Item	$p_T$	$ \eta $
$\ell^\pm$	$\geq 15$ GeV	$\leq 2$
MET ( $\nu$ )	$\geq 15$ GeV	-
jet ( $b$ -tag)	$\geq 20$ GeV	$\leq 2$
jet (no $b$ -tag)	$\geq 20$ GeV	$\leq 3.5$
	Min	Max
$H_T$	$\geq 180$ GeV	$\leq 250$ GeV
" $m_t$ "	$\geq 160$ GeV	$\leq 190$ GeV

TABLE II: Representative “intermediate” cuts.

combination thereof) has the lowest theoretical uncertainties has not been resolved and we will not attempt to answer this very important question definitively here. For this study we have chosen to cut on the quantity

$$H_T = \sum_{\text{jets}} (p_T)_i + (p_T)_\ell + \cancel{E}_T ,$$

where the sum is over all jets with  $p_T > 20$  GeV and  $|\eta| < 3.5$ ,  $(p_T)_i$  is the magnitude of the transverse momentum of the  $i^{\text{th}}$  jet,  $(p_T)_\ell$  that of the lepton, and  $\cancel{E}_T$  is the missing transverse energy in the event. Large values of  $H_T$  tend to favor  $t\bar{t}$  final states, while lower values favor  $Wj^n$  final states, with the signal contribution peaking at intermediate values.

Furthermore, since the signal involves a  $t$ -quark, we also impose a requirement that the invariant mass of the lepton, neutrino, and the leading tagged jet be approximately equal to the top quark mass. In doing so, we must reconstruct the neutrino’s momentum  $p_{\nu,z}$  along the beam axis, which has an ambiguity. We require that  $(p_\ell + p_\nu)^2 = m_W^2$ , and among the two solutions for  $p_{\nu,z}$  we choose the solution with smallest absolute magnitude. (For complex solutions, only the real part is used.)

As suggested earlier, we find that such cuts cannot decrease the backgrounds to the point that they are comparable to the signal. Two choices of “intermediate” and “hard” cuts are indicated in Tables II and III. The resulting numbers of expected events for an integrated luminosity of  $3 \text{ fb}^{-1}$ , summing over  $e^\pm$  and  $\mu^\pm$  (and thus including both  $t$  and  $\bar{t}$ ), can be seen in Table IV. We show the number of events which survive both the basic cuts of Table I, the intermediate cuts of Table II, and the hard cuts of Table III. Consistent with [1], we find that while all of the cuts contribute to the background reduction, the  $Wj^n$  channel is reduced primarily by a combination of the stiffer  $p_T$  cuts and the “ $m_t$ ” cut, while the  $t\bar{t}$  background is affected primarily by the upper  $H_T$  cut. While the basic cuts reveal a signal to background ratio of approximately 1:21, this improves to 1:7.4 and 1:4.9 using the intermediate and hard cuts. This is, at best, disappointing.

The difference in the results between our study and that of [1] is striking, and requires an explanation.<sup>3</sup> We believe the main effects can be accounted for straightforwardly. First, in the present study we have the benefit of recent

---

<sup>3</sup> Due to our different cuts and somewhat different approaches, a detailed comparison between the results of the two analyses is difficult. To obtain some quantitative sense of the differences let us focus on the ratio of signal ( $tbq + tb$ ) to  $Wjj$  background, which is where the bulk of the difference arises and which provides an upper limit on the full signal to background ratio. For example, consider this ratio for the “basic cuts” results in Table IV yielding a ratio of 0.065. This is most usefully compared with the middle column (without parentheses) in Table 3 of [1], where the corresponding ratio is 0.24. The factor of nearly 4 difference results primarily from our much larger estimate of the  $Wjj$  contribution (larger by more than a factor of 3). Adding the  $m_t$  cut in [1] increases their value for the ratio

Item	$p_T$	$ \eta $
$\ell^\pm$	$\geq 15$ GeV	$\leq 2$
MET ( $\nu$ )	$\geq 15$ GeV	-
jet ( $b$ -tag)	$\geq 60$ GeV	$\leq 2$
jet (no $b$ -tag)	$\geq 30$ GeV	$\leq 3.5$
	Min	Max
$H_T$	$\geq 180$ GeV	$\leq 250$ GeV
$m_t$	$\geq 160$ GeV	$\leq 190$ GeV

TABLE III: Representative “hard” cuts.

Channel	Basic Cuts	“Intermediate ” Cuts	“Hard” Cuts
$tbq$	298	67	30
$tb$	145	27	13
$t\bar{t}$	2623	140	57
$Wjj$	6816	550	152
$(tbq + tb) / (t\bar{t} + Wjj)$	0.047	0.14	0.21

TABLE IV: Numbers of events for  $3 \text{ fb}^{-1}$  (summed over  $t$  and  $\bar{t}$ ,  $e$  and  $\mu$  channels) for the three sets of cuts in Tables I–III.

next-to-leading-order calculations [18], which increase the overall rate for  $Wj^n$  by of order 50 % compared to that used in [1]. (In our leading-order computations, this is effectively obtained through our lower choice of renormalization scale.) Second, we find a much larger number of tagged jets in the  $Wj^n$  channel, because we include (by simulating parton showering) the fragmentation of leading-order partonic gluons into heavy flavor jets at subleading orders. (This effect would appear already in a next-to-leading-order calculation, such as performed recently in [9].) Third, our more pessimistic estimate of energy resolution at the Fermilab detectors forces us to use a wider  $m_t$  window cut in order to have sufficient acceptance for the signal; this lets in more  $Wj^n$  background. Fourth, we use a more pessimistic  $b$ -tagging rate (50% *vs* 60%) and light-quark-jet mistagging rate (1.0% *vs* 0.5%), a more pessimistic charm-to-bottom ratio in tagging (1:3.3 *vs* 1:4.0), and more realistic  $p_T$  distributions in tagging functions; these all hurt the signal-to-background ratio and the efficiency for the signal. Other small negative effects include a lower center of mass energy (1.96 TeV *vs.* 2.00 TeV), and a lower cross-section for the signal (due largely to a change in parton distribution functions.) Note also that we have used  $m_t = 175$  GeV, so our results may even be slightly optimistic in this regard.

The numbers in Table IV suggest that a further factor of 3–5 improvement in the signal-to-background ratio via more aggressive cuts will come at the cost of a factor of 5–10 reduction in the signal accompanied by a factor of 15–45 reduction in the background. The essential question then is whether a reduction by such a large factor can be achieved without large systematic and theoretical errors. From Table IV, one can see that systematic errors below about 10% in  $Wj^n$  are needed for a discovery. Unfortunately, the method for removing the background suggested in [1], namely, to use a jet veto to reduce  $t\bar{t}$  to a small contribution, and do a sideband analysis on either side of the  $m_t$  window cut to remove  $Wj^n$ , is unlikely to work with such a large  $Wj^n$  background. This is illustrated in Fig. 2. With basic cuts, the  $Wj^n$  background (whose “ $m_t$ ” distribution falls steeply and monotonically above 125 GeV) is very large, as shown in Fig. 2a. A sideband analysis with a window centered around 175 GeV would be subject to large statistical errors. Meanwhile, the intermediate and hard cuts, shown in Figs. 2b and 2c, tend to shape the  $Wj^n$  events such that the  $Wj^n$  background is no longer monotonic near and/or across the  $m_t$  window, making a sideband analysis problematic. Thus the shape of the “ $m_t$ ” distribution of the  $Wj^n$  background after hard cuts must be predicted, with small errors. We will argue later that this is very difficult. Consequently, we doubt that a straightforward counting experiment can yield, on its own, a satisfactory measurement of the cross-section for the production of single top.

---

to 0.77. However, with our much larger  $Wjj$  contribution, we can improve this ratio to only 0.28 when using the “hard” cuts that include a cut on  $m_t$ , *i.e.*, the factor of 3 larger  $Wjj$  background is still there. The jet veto used in [1] (the last column in their Table 3) only reduces the background from  $t\bar{t}$  (and also the signal), and does not help reduce the  $Wjj$  background.

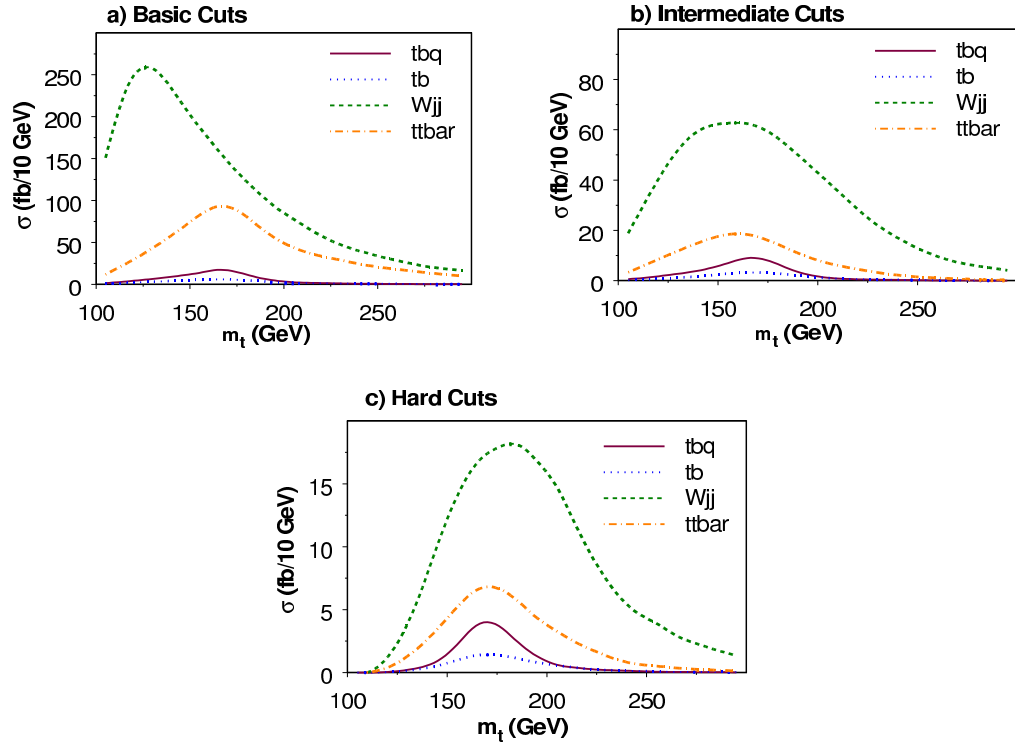


FIG. 2: Distribution of the reconstructed “ $m_t$ ”, the invariant mass of the charged lepton, neutrino and highest- $p_T$   $b$ -tagged jet, for the backgrounds and signals. Additional details concerning the construction of this observable are given in the text. The three figures show the results for the (a) basic, (b) intermediate and (c) hard cuts given in Tables I-III, with the cut on “ $m_t$ ” omitted.

## B. Shape Variables

Under the assumption that a counting experiment is insufficient, we turn to observables that (as in [4, 6]) make use of other aspects of the signal. In particular, we will now explore variables that take advantage of the very special shape of single top production compared to the background, and are less subject to, or less sensitive to, systematic errors.

As noted earlier, the dominant production process is  $tbq$ , in which there is a hard lepton, and also a hard untagged jet  $j$  with pseudo-rapidity  $|\eta| \sim 1 - 3$  and  $p_T$  typically larger than 25 GeV. This strongly forward or backward jet is a distinctive signature which the backgrounds do not share. The  $b$  jet from the  $t$  decay tends to be produced centrally (low pseudo-rapidity) with high- $p_T$ , and is typically the tagged jet (for which reason we only use the tagged jet in the  $t$  reconstruction.) The other  $b$  jet tends to have low  $p_T$ ; it is often unobserved, and is rarely tagged [1].

Importantly, the  $tbq$  process arises from an initial state light quark or antiquark (typically a valence quark carrying moderate to large Bjorken- $x$ ) scattering off a gluon (typically carrying lower  $x$ .) This unusual initial state has important kinematic consequences. Because of this kinematic effect, the structure of the proton, and the details of the electroweak theory, the  $tbq$  signal has strong and distinctive correlations and asymmetries which we can use to separate it from the backgrounds.

First, the unusual kinematics and the structure of the proton combine in an interesting way. The creation of positively-charged top quarks (and consequently positively-charged leptons in the final state) in the  $t\bar{b}q$  process requires either a  $u$  or  $\bar{d}$  in the initial state, so that a  $W^+$  can be emitted from the quark line. Since a reasonably large value of Bjorken- $x$  is necessary in order to produce the top quark, the required initial state is most often obtained from a valence quark striking a gluon. The most likely initial state uses a valence  $u$  quark from the  $p$ ; the next most likely draws a valence  $\bar{d}$  from the  $\bar{p}$ , and thereafter we must draw on the sea quarks from either  $p$  or  $\bar{p}$ . Since the quark usually has larger  $x$  than the gluon that it strikes, the  $t\bar{b}q$  system is typically boosted in the direction of travel of the

initial quark. Consequently, for  $t$  quarks, the  $t\bar{b}q$  system is more likely to be boosted in the proton direction than in that of the antiproton, by a factor of roughly 2:1. The reverse is true for  $\bar{t}$  production. Moreover, the light-quark jet in the final state, converted from the quark in the initial state by the emission of the  $W$ , tends to travel in the proton direction when a  $t$  is produced and in the antiproton direction when a  $\bar{t}$  is produced.

Thus, because of the differences between the  $u$  and  $d$  parton distribution functions in the proton, and because of the quark-gluon initial state, large asymmetries under parity  $P$  and charge conjugation  $C$  result. These show up strongly in the differential cross-section both for the top (and the positively charged lepton in its decays) and for the hard forward or backward light-quark jet.

Second, the momentum vectors of the lepton and the light-quark jet are correlated, as a result of both kinematics and spin polarization effects. The structure of the electroweak interactions ensures that the spin of the top quark tends to align with the momentum direction of the light-quark jet. Since the top decays before this spin information is lost, it is transferred to the momentum of the final-state charged lepton. In the  $t$  rest frame the lepton momentum and jet momentum tend to align [20]. The boost of the top quark relative to the lab frame, whose sign is also aligned with the momentum direction of the jet, further tends to push both lepton and jet into the same hemisphere.

These properties strongly distinguish the  $tbq$  process from its  $t\bar{t}$  background. At tree-level,  $t\bar{t}$  is separately  $C$  and  $P$  invariant. Clearly this is true of the process  $gg \rightarrow t\bar{t}$ , since the initial state is  $P$ -invariant on average. It is also true of the process  $q\bar{q} \rightarrow g \rightarrow t\bar{t}$ , because the intermediate gluon state is a  $C$ -eigenstate; this is the same as in  $e^+e^- \rightarrow \mu^+\mu^-$ , where there is no forward-backward asymmetry in the  $\mu^+$  distribution. The parity-invariance is violated at the next order, due to radiative effects [21]; this is a few percent effect, both small and calculable. Moreover, there should be no strong correlation between the momenta of the lepton and the jets in the final state. In those  $t\bar{t}$  events which have both low  $H_T$  and a reconstructable semileptonically-decaying top quark, one or two jets from the hadronically-decaying top tend to be lost or mismeasured. Meanwhile any high- $p_T$  untagged jets whose momenta we might choose to compare with that of the lepton will also stem from the hadronically-decaying top. The accidents which lead to the selection of any given jet as part of our analysis should largely wash out any correlation of its momentum with that of the lepton. Indeed, our simulations show that in  $t\bar{t}$  the correlation between the lepton and the highest- $p_T$  untagged jet (which we will use in our analysis below) is roughly a 10% effect.

Similar considerations apply, to a good approximation, to those QCD events which might pass our cuts. Parity asymmetries for these events are small. The charge of a fake leptons is unrelated to its momentum direction. Consequently, all distributions for events with fake leptons are invariant under flipping the sign of the lepton charge; as we will see, this implies that these events have  $P$ -invariant distributions for the observables we will choose. Isolated leptons from heavy flavor stem mainly from  $c\bar{c}$  and  $b\bar{b}$  events; these have similar  $C$  and  $P$  properties to  $t\bar{t}$ , so we expect small parity-asymmetries. Meanwhile, a fake lepton and the highest- $p_T$  untagged jet in the event should be essentially uncorrelated. However, if this jet contains heavy flavor, then a correlation can arise when the lepton observed in the event is from a wide-angle semileptonic decay of a heavy-quark within the jet. The precise size of jet-lepton correlations from this source is unknown to us, and is detector- and cut-dependent. The small overall number of QCD events entering the single top samples at DZero [7] suggests that QCD contributions to jet-lepton correlations are not a major issue for the single top measurement, except possibly in the case of muons from heavy flavor decays. We will return to this possible exception in section III.D.

The parity asymmetry in  $Wj^n$  unfortunately has the same sign as that of  $tbq$ , although it is less pronounced. The reasons for this are easy to see. As with a  $t$  quark, a  $W^+$  is most likely to be produced moving in the proton direction, since it is most often produced in a  $u\bar{d}$  event. This leads to a well-known asymmetry in its pseudo-rapidity. When produced in conjunction with two jets, the  $W^+$  still tends to be boosted in the proton direction, since its initial state is most often  $ug$  or  $u\bar{d}$ . This leads to parity asymmetries which, though relatively small, are still quite large in absolute size compared to the signal.<sup>4</sup> Unfortunately, the size of the asymmetries and correlations in  $Wj^n$  appears to be very sensitive to assumptions, cuts, Monte Carlo parameters, and tagging, and will be a source of significant systematic error. We will return to this issue later.

### C. Consequences of Parity and Correlations

In order to make the best use of these special properties of the signals and backgrounds, it is useful to consider these issues more formally. We next discuss the effect of  $C$  and  $P$  (non)-invariance, and of lepton-jet pseudo-rapidity

---

<sup>4</sup> Note these asymmetries in pseudo-rapidity, or equivalently angle, for fixed charge, are due to the Tevatron's proton-antiproton initial state. At the LHC, with a proton-proton initial state, the same effects will show up as *charge* asymmetries for fixed angle.



correlations, on two-dimensional distributions in pseudo-rapidity. The “jet” used throughout the analysis below is always *the highest- $p_T$  untagged jet* in the event.

The  $p\bar{p}$  initial state of the Tevatron is a CP eigenstate, and so all distributions of final state particles are CP-invariant (to an excellent approximation, violated principally by the detector). This means that the differential cross-section  $d^2\sigma^+/d\eta_j d\eta_\ell$  with respect to the rapidities of the jet and the positively charged lepton, and the corresponding distribution  $d^2\sigma^-/d\eta_j d\eta_\ell$  for processes with a *negatively* charged lepton, *must* be related by CP:

$$\frac{d^2\sigma^+}{d\eta_j d\eta_\ell}(\eta_j, \eta_\ell) = \frac{d^2\sigma^-}{d\eta_j d\eta_\ell}(-\eta_j, -\eta_\ell) .$$

Consequently, we can combine data from positively and negatively charged leptons by defining a *lepton-charge-weighted pseudo-rapidity*,  $\hat{\eta}_j = Q_\ell \eta_j$ ,  $\hat{\eta}_\ell = Q_\ell \eta_\ell$ , where  $Q_\ell$  is the lepton charge. (The variable  $\hat{\eta}_j$  was already introduced in [4, 6].) For the remainder of this article, our entire discussion is based on the explicitly CP-invariant differential cross section

$$\frac{d^2\sigma}{d\hat{\eta}_j d\hat{\eta}_\ell}(\hat{\eta}_j, \hat{\eta}_\ell) \equiv \frac{d^2\sigma^+}{d\eta_j d\eta_\ell}(\eta_j = \hat{\eta}_j, \eta_\ell = \hat{\eta}_\ell) + \frac{d^2\sigma^-}{d\eta_j d\eta_\ell}(\eta_j = -\hat{\eta}_j, \eta_\ell = -\hat{\eta}_\ell) .$$

However, the  $p\bar{p}$  initial state is not an eigenstate of either C or P. Consequently, in general we expect parity-non-invariance

$$\frac{d^2\sigma^+}{d\eta_j d\eta_\ell}(\eta_j, \eta_\ell) \neq \frac{d^2\sigma^+}{d\eta_j d\eta_\ell}(-\eta_j, -\eta_\ell) ,$$

and similar non-invariance under charge conjugation

$$\frac{d^2\sigma^+}{d\eta_j d\eta_\ell}(\eta_j, \eta_\ell) \neq \frac{d^2\sigma^-}{d\eta_j d\eta_\ell}(\eta_j, \eta_\ell) .$$

(Indeed these two statements are equivalent due to CP-invariance.) In terms of the combined differential cross-section, P (and C) non-invariance implies

$$\frac{d^2\sigma}{d\hat{\eta}_j d\hat{\eta}_\ell}(\hat{\eta}_j, \hat{\eta}_\ell) \neq \frac{d^2\sigma}{d\hat{\eta}_j d\hat{\eta}_\ell}(-\hat{\eta}_j, -\hat{\eta}_\ell) .$$

Conversely, if we were to study a *parity-symmetric* process, such as the tree-level production of  $t\bar{t}$ , it would satisfy

$$\frac{d^2\sigma}{d\hat{\eta}_j d\hat{\eta}_\ell}(\hat{\eta}_j, \hat{\eta}_\ell) = \frac{d^2\sigma}{d\hat{\eta}_j d\hat{\eta}_\ell}(-\hat{\eta}_j, -\hat{\eta}_\ell) \quad (\text{parity} - \text{even process}) .$$

Next, let us consider the effect of correlations. If the dynamics of a process is such that the jet and lepton directions are uncorrelated, then the differential cross-section factorizes into a product of two distributions, one for the jet and one for the lepton:

$$\frac{d^2\sigma}{d\hat{\eta}_j d\hat{\eta}_\ell} = f(\hat{\eta}_j)g(\hat{\eta}_\ell) \quad (\text{jet and lepton uncorrelated}) .$$

Failure of this relation is proof of correlations. These might stem directly from correlations in the rest frame of the  $tbq$  system. However, even if the distributions in the rest frame are uncorrelated, they will be correlated in the lab frame, once they are convolved with a distribution of boosts of the rest frame.<sup>5</sup>

---

<sup>5</sup> For example, suppose  $\frac{d^2\sigma}{d\hat{\eta}_j d\hat{\eta}_\ell} = f(\hat{\eta}_j)g(\hat{\eta}_\ell)$  in the  $tbq$  rest frame, with Gaussian lepton and jet distributions:

$$f(\hat{\eta}_j) \propto e^{-A_j \hat{\eta}_j^2}, \quad g(\hat{\eta}_\ell) \propto e^{-A_\ell \hat{\eta}_\ell^2}$$

Suppose further that the rest frame is boosted by an amount  $\eta_b$  with a propability which also has a Gaussian distribution

$$p(\eta_b) \propto e^{-B\eta_b^2}$$

Then the observed distribution in the lab frame is

$$\frac{d\sigma}{d\hat{\eta}_j d\hat{\eta}_\ell} \propto \int_{-\infty}^{\infty} d\eta_b f(\hat{\eta}_j - \eta_b) g(\hat{\eta}_\ell - \eta_b) p(\eta_b) \propto e^{-[(B+A_\ell)A_j \hat{\eta}_j^2 + (B+A_j)A_\ell \hat{\eta}_\ell^2 - A_j A_\ell \hat{\eta}_j \hat{\eta}_\ell] / (A_j + A_\ell + B)} .$$

This is a correlated distribution; it cannot be written as  $F(\eta_j)G(\eta_\ell)$ , because of the cross-term in the exponent. Note the correlation vanishes in the limit of a very narrow distribution of boosts,  $B \rightarrow \infty$ , even if the boost distribution is not centered at zero.

Item	$p_T$	$ \eta $
$\ell^\pm$	$\geq 15$ GeV	$\leq 2$
MET ( $\nu$ )	$\geq 15$ GeV	-
jet ( $b$ -tag)	$\geq 40$ GeV	$\leq 2$
jet (no $b$ -tag)	$\geq 30$ GeV	$\leq 3.5$
	Min	Max
$H_T$	none	$\leq 300$ GeV
" $m_t$ "	$\geq 155$ GeV	$\leq 200$ GeV

TABLE V: "Relaxed" cuts for analysis.

Finally, if the process is both uncorrelated *and* P-invariant, then both distributions must be even functions of their particle's pseudo-rapidity. In short

$$\frac{d^2\sigma}{d\hat{\eta}_j d\hat{\eta}_\ell} = f(\hat{\eta}_j)g(\hat{\eta}_\ell) ; f(\hat{\eta}_j) = f(-\hat{\eta}_j) ; g(\hat{\eta}_\ell) = g(-\hat{\eta}_\ell) \quad (\text{uncorrelated, parity} - \text{even}) .$$

with the four-way consequence

$$\frac{d^2\sigma}{d\hat{\eta}_j d\hat{\eta}_\ell}(\hat{\eta}_j, \hat{\eta}_\ell) = \frac{d^2\sigma}{d\hat{\eta}_j d\hat{\eta}_\ell}(-\hat{\eta}_j, -\hat{\eta}_\ell) = \frac{d^2\sigma}{d\hat{\eta}_j d\hat{\eta}_\ell}(\hat{\eta}_j, -\hat{\eta}_\ell) = \frac{d^2\sigma}{d\hat{\eta}_j d\hat{\eta}_\ell}(-\hat{\eta}_j, \hat{\eta}_\ell) \quad (1)$$

for such processes.<sup>6</sup> The  $t\bar{t}$  process does indeed satisfy the relation (1) at the 90% level. We believe this continues to next-to-leading order: one-loop effects cause a 5% parity asymmetry in  $t$  and  $\bar{t}$  production angles [21], which, when translated into jet and lepton pseudo-rapidities, is unlikely to violate parity by more than 10% (though this has not been simulated for our specific cuts.) We believe that QCD contributions to the sample are similarly in good agreement with (1), except possibly for lepton-jet correlations in events with heavy flavor. The  $Wj^n$  background, with its moderate asymmetries and correlations, accords with (1) only to a very rough approximation. And as we have emphasized, the  $tbq$  signal strongly violates the relation (1).

#### D. Strategy and Tactics

To illustrate the characteristic properties of the various channels, we will study a simulated event sample defined by the cuts in Table V. These cuts are more "relaxed" than those of Tables II and III, keeping a larger fraction of both the signal and the background, and yielding a sample which we believe is less sensitive to the systematic uncertainties stemming from the cuts. We will argue below that shape considerations will allow us to make some headway toward separating signal and background. The simulated differences in shape are summarized in the contour plots of Fig. 3, which give the distributions ( $d^2\sigma/d\hat{\eta}_j d\hat{\eta}_\ell$ ) of the various processes, plotted as functions on the  $(\hat{\eta}_j, \hat{\eta}_\ell)$  plane. (Recall that we define the "jet" of relevance to be the highest- $p_T$  untagged jet.)

Figure 3 illustrates the degree to which the various processes exhibit correlations and asymmetries. We label the four quadrants of the  $(\hat{\eta}_j, \hat{\eta}_\ell)$  plane A, B, C, D as shown in Fig. 4. Positive jet-lepton correlations cause events to pile up in quadrants B and C, while parity asymmetries appear in the differences between quadrants B and C, and between quadrants A and D. The  $tbq$  signal in Fig. 3b shows clearly shows both effects. The  $Wj^n$  background, in Fig. 3d, also has an asymmetric shape, though to a lesser relative degree. The  $t\bar{t}$  process, Fig. 3a, shows some correlation but no asymmetry, while Fig. 3c illustrates the uncorrelated and symmetric nature of (tree-level)  $t\bar{t}$ .

As a quantitative measure of these statements, we consider the differential cross-sections integrated separately over the four quadrants of the  $(\hat{\eta}_j, \hat{\eta}_\ell)$  plane. For a given luminosity  $\mathcal{L}$ , the number of  $tbq$  events in the A quadrant is

$$\mathcal{L} \times \int_0^2 d\hat{\eta}_\ell \int_{-3.5}^0 d\hat{\eta}_j \frac{d^2\sigma^{tbq}}{d\hat{\eta}_j d\hat{\eta}_\ell} ,$$

<sup>6</sup> Note the logic is not reversible; a distribution satisfying the condition (1) is not necessarily uncorrelated.

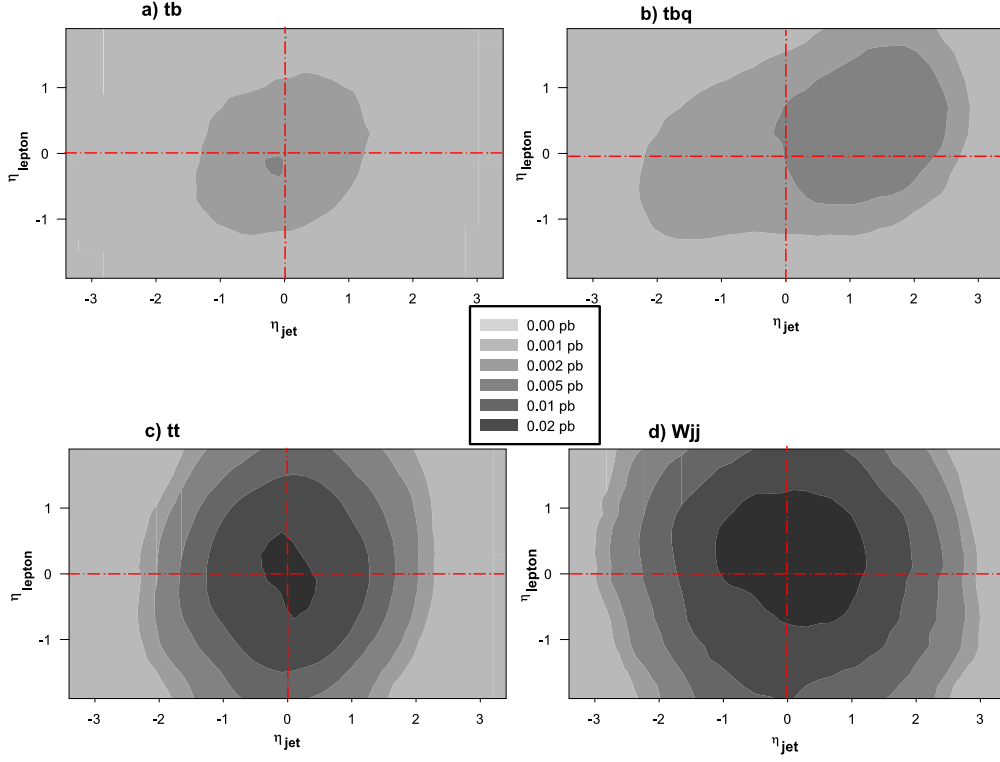


FIG. 3: Differential cross-section ( $d^2\sigma/d\hat{\eta}_j d\hat{\eta}_\ell$ , summed over  $t$  and  $\bar{t}$ ,  $e$  and  $\mu$ ) for the a)  $tb$  channel b)  $tbq$  channel, c)  $t\bar{t}$  channel, and d)  $Wjj$  channel, after  $b$ -tagging and the cuts of Table V.

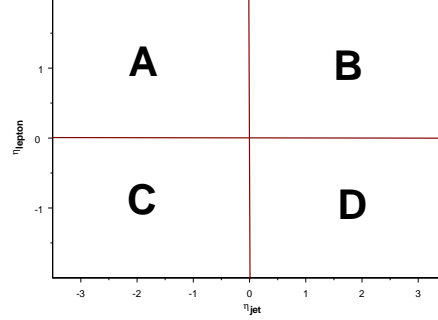


FIG. 4: The four quadrants of the  $(\hat{\eta}_j, \hat{\eta}_\ell)$  plane.

Channel	A	B	C	D
$tb$	8	11	12	8
$tbq$	14	41	18	22
$t\bar{t}$	105	109	106	105
$Wjj$	204	207	159	180

TABLE VI: Numbers of events for  $3 \text{ fb}^{-1}$  in the four quadrants for various channels (summed over  $t$  and  $\bar{t}$ ,  $e$  and  $\mu$ ). See Fig. 4 for definition and labels of the quadrants.

that in the B quadrant is

$$\mathcal{L} \times \int_0^2 d\hat{\eta}_\ell \int_0^{3.5} d\hat{\eta}_j \frac{d^2\sigma^{tbq}}{d\hat{\eta}_j d\hat{\eta}_\ell},$$

and so forth. The resulting numbers of events with  $\mathcal{L} = 3 \text{ fb}^{-1}$  of data appear in Table VI (summed over  $t$  and  $\bar{t}$ ,  $e$  and  $\mu$ ). Statistical uncertainties in each bin are uncorrelated with other bins. Systematic uncertainties in these numbers, which are very substantial for  $Wj^n$ , deserve considerable discussion; since this table is merely intended for a general illustration, we defer this discussion until Sec. IV.

To capture quantitatively these differences in shape between signal and background, we suggest defining three orthogonal functions in the  $(\hat{\eta}_j, \hat{\eta}_\ell)$  plane, based on the formal discussion of the previous section. For any differential cross-section, whether a signal, a background or a combination, and whether simulated or measured experimentally, we may write it as a sum of three components

$$\frac{d^2\sigma}{d\hat{\eta}_j d\hat{\eta}_\ell}(\hat{\eta}_j, \hat{\eta}_\ell) = \bar{F}(\hat{\eta}_j, \hat{\eta}_\ell) + F_+(\hat{\eta}_j, \hat{\eta}_\ell) + F_-(\hat{\eta}_j, \hat{\eta}_\ell), \quad (2)$$

where the components are of the form

$$\bar{F}(\hat{\eta}_j, \hat{\eta}_\ell) \equiv \frac{1}{4} \left[ \frac{d^2\sigma}{d\hat{\eta}_j d\hat{\eta}_\ell}(\hat{\eta}_j, \hat{\eta}_\ell) + \frac{d^2\sigma}{d\hat{\eta}_j d\hat{\eta}_\ell}(-\hat{\eta}_j, -\hat{\eta}_\ell) + \frac{d^2\sigma}{d\hat{\eta}_j d\hat{\eta}_\ell}(\hat{\eta}_j, -\hat{\eta}_\ell) + \frac{d^2\sigma}{d\hat{\eta}_j d\hat{\eta}_\ell}(-\hat{\eta}_j, \hat{\eta}_\ell) \right] \quad (3)$$

$$F_+(\hat{\eta}_j, \hat{\eta}_\ell) \equiv \frac{1}{4} \left[ \frac{d^2\sigma}{d\hat{\eta}_j d\hat{\eta}_\ell}(\hat{\eta}_j, \hat{\eta}_\ell) + \frac{d^2\sigma}{d\hat{\eta}_j d\hat{\eta}_\ell}(-\hat{\eta}_j, -\hat{\eta}_\ell) - \frac{d^2\sigma}{d\hat{\eta}_j d\hat{\eta}_\ell}(\hat{\eta}_j, -\hat{\eta}_\ell) - \frac{d^2\sigma}{d\hat{\eta}_j d\hat{\eta}_\ell}(-\hat{\eta}_j, \hat{\eta}_\ell) \right] \quad (4)$$

$$F_-(\hat{\eta}_j, \hat{\eta}_\ell) \equiv \frac{1}{2} \left[ \frac{d^2\sigma}{d\hat{\eta}_j d\hat{\eta}_\ell}(\hat{\eta}_j, \hat{\eta}_\ell) - \frac{d^2\sigma}{d\hat{\eta}_j d\hat{\eta}_\ell}(-\hat{\eta}_j, -\hat{\eta}_\ell) \right] \quad (5)$$

Let us comment on some properties of these functions. First, they are explicit functions, not abstract devices: they can be directly constructed from any finite data set, simulated or measured. Second, they are orthogonal in the sense that

$$\int_{-a}^a d\hat{\eta}_j \int_{-b}^b d\hat{\eta}_\ell \bar{F} F_\pm = 0 ; \int_{-a}^a d\hat{\eta}_j \int_{-b}^b d\hat{\eta}_\ell F_+ F_- = 0 ;$$

(where  $a$  and  $b$  are arbitrary positive numbers); indeed this orthogonality applies in any symmetrically-defined region of the  $(\hat{\eta}_j, \hat{\eta}_\ell)$  plane. Third, the functions provide important physical information about the symmetry properties of the differential cross-section.  $\bar{F}$  and  $F_+$  are parity-even while  $F_-$  is parity-odd; thus  $F_- = 0$  (within statistics) for any parity-even distribution. Meanwhile, because of Eq. (1),  $F_+$  will also vanish if the distribution is parity-even *and* the leptons and jets are uncorrelated. Fourth, by construction, these functions have special symmetries under reflection in the  $(\hat{\eta}_j, \hat{\eta}_\ell)$  plane, as will be obvious in the figures below.  $\bar{F}$  and  $F_+$  have four-way symmetry; in both cases, it is sufficient to know the function in any one quadrant to know it in all four quadrants. Meanwhile  $F_-$  has two-way symmetry; quadrants A and D are related, as are B and C, but quadrants A and B are independent and must be determined separately.<sup>7</sup>

In the problem at hand, the fact that the signal has strong asymmetries and correlations, while the backgrounds do not, is very usefully characterized using these functions. In particular, we expect, based on the properties we have discussed above, that

$$\bar{F}^{t\bar{t}} \gg |F_\pm^{t\bar{t}}| ; \bar{F}^{Wj^n} > |F_\pm^{Wj^n}| ; \bar{F}^{tbq} \sim |F_\pm^{tbq}| .$$

Our simulations further suggest that one can find cuts that are feasible at the Tevatron such that the backgrounds are still very large but only in  $\bar{F}$ , with

$$\bar{F}^{t\bar{t}} \sim \bar{F}^{Wj^n} \gg \bar{F}^{tbq} ,$$

---

<sup>7</sup> In short,  $F_-$  contains twice as much information as  $F_+$  and  $\bar{F}$ . In principle one could further separate  $F_-$  into two orthogonal functions, but this turns out not to be particularly useful.

while the signal has a much larger role to play in the other functions:

$$|F_+^{t\bar{t}}| \sim |F_+^{Wj^n}| \sim |F_+^{tbq}|, \quad |F_-^{t\bar{t}}| \ll |F_-^{Wj^n}| \sim |F_-^{tbq}|.$$

especially away from the center of the  $(\hat{\eta}_j, \hat{\eta}_\ell)$  plane. (The  $tb$  signal is smaller than the  $tbq$  signal for all quantities, but especially for  $F_+$ , by a factor of about 3, and for  $F_-$ , by a factor of order 10.)

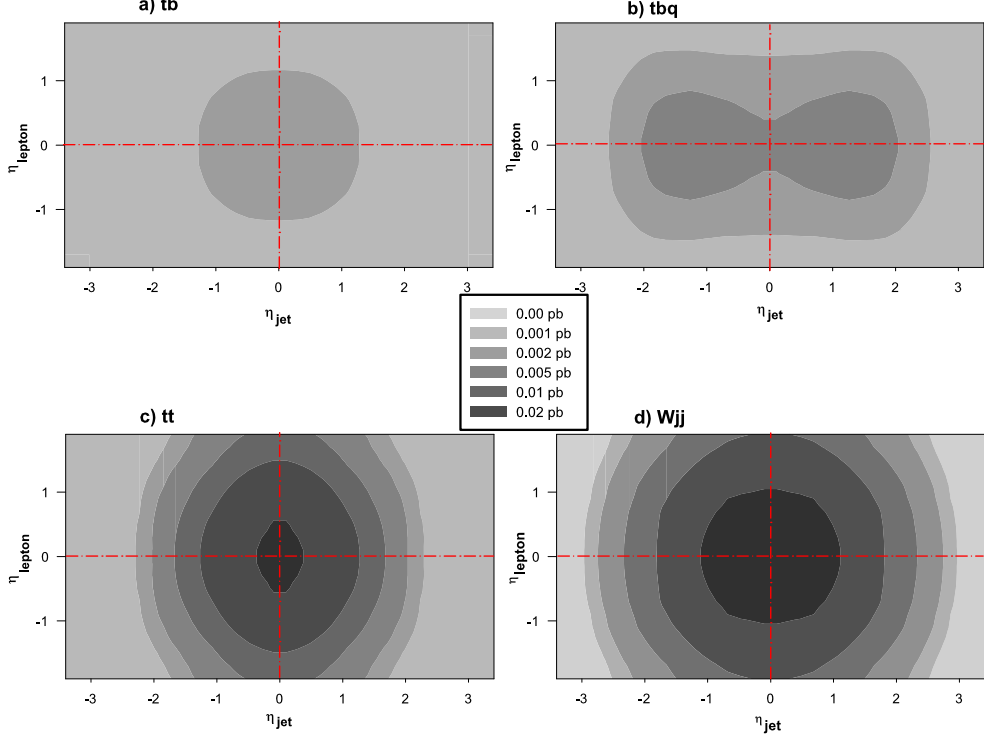


FIG. 5: Contour plots for the function  $\bar{F}(\hat{\eta}_j, \hat{\eta}_\ell)$  for a)  $tb$ , b)  $tbq$ , c)  $t\bar{t}$ , and d)  $Wjj$  channels (summed over  $t$  and  $\bar{t}$ ,  $e$  and  $\mu$ ).

These claims are illustrated in Figs. 5, 6 and 7, where the functions  $\bar{F}$ ,  $F_+$ ,  $F_-$  are shown, for  $tb$ ,  $tbq$ ,  $t\bar{t}$ , and  $Wj^n$ . (The reader should note that the scale for the contours in Figs. 6 and 7 differs from that used in Figs. 3 and 5; this is because of the smaller dynamic range in the  $F_\pm$  distributions.) The symmetry properties of the three functions discussed earlier are clearly evident.

To make this comparison more concrete, the integrals of the 3 functions over quadrants A and B, for an integrated luminosity  $\mathcal{L} = 3 \text{ fb}^{-1}$ , are presented in Table VII; this table can be constructed from Table VI. The definitions of the entries in the table are

$$\begin{aligned} \bar{F}_A &\equiv \mathcal{L} \times \int_A d\hat{\eta}_j d\hat{\eta}_\ell \bar{F} = \bar{F}_B = \bar{F}_C = \bar{F}_D, \\ F_{+,A} &\equiv \mathcal{L} \times \int_A d\hat{\eta}_j d\hat{\eta}_\ell F_+ = -F_{+,B} = -F_{+,C} = F_{+,D}, \\ F_{-,A} &\equiv \mathcal{L} \times \int_A d\hat{\eta}_j d\hat{\eta}_\ell F_- = -F_{-,D}, \\ F_{-,B} &\equiv \mathcal{L} \times \int_B d\hat{\eta}_j d\hat{\eta}_\ell F_- = -F_{+,C}. \end{aligned}$$

The table also shows the statistical errors in these quantities. Since this table is intended only to emphasize qualitative points, we postpone discussion of systematic errors and next-to-leading order corrections until we outline a more sophisticated approach with better statistical errors.

As we argued before, we are justified in disregarding QCD events. The number of QCD events entering the sample is small [7],

$$\bar{F}^{t\bar{t}}, \bar{F}^{Wj^n} \gg \bar{F}^{QCD} \sim \bar{F}^{tbq}, \bar{F}^{tb}.$$

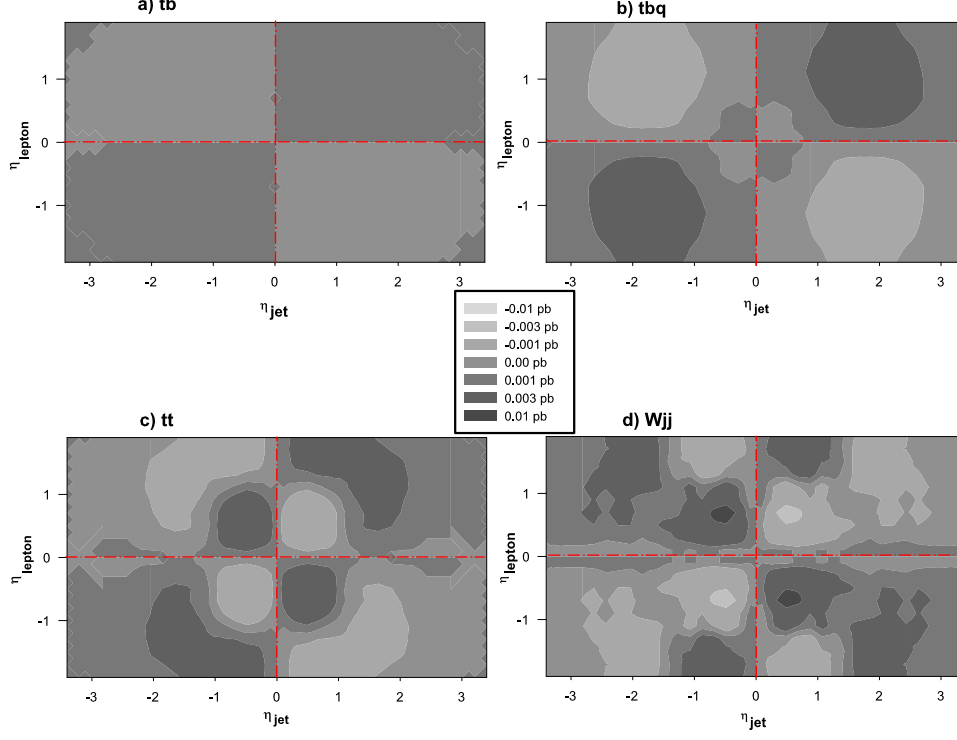


FIG. 6: Contour plots for the function  $F_+$  ( $\hat{\eta}_j, \hat{\eta}_\ell$ ) for a)  $tb$ , b)  $tbq$ , c)  $t\bar{t}$ , and d)  $Wjj$  channels (summed over  $t$  and  $\bar{t}$ ,  $e$  and  $\mu$ ).

Channel	$\overline{F}_A = \overline{F}_B$	$F_{+,B} = -F_{+,A}$	$F_{-,A}$	$F_{-,B}$
$tb$	$9.8 \pm 1.6$	$1.4 \pm 1.6$	$0.0 \pm 2.1$	$-0.3 \pm 2.4$
$tbq$	$23.8 \pm 2.4$	$5.6 \pm 2.4$	$-3.7 \pm 3.0$	$11.6 \pm 3.8$
$t\bar{t}$	$106.1 \pm 5.2$	$1.2 \pm 5.2$	$-0.2 \pm 7.2$	$1.3 \pm 7.3$
$Wjj$	$187.7 \pm 6.9$	$-4.6 \pm 6.9$	$11.8 \pm 9.8$	$23.8 \pm 9.6$

TABLE VII: Numbers of events for  $3 \text{ fb}^{-1}$  in  $\overline{F}$ ,  $F_+$  and  $F_-$ , integrated over quadrants A and B, for the various channels (summed over  $t$  and  $\bar{t}$ ,  $e$  and  $\mu$ ). Errors shown are statistical only. See text for further interpretation.

For the DZero detector, the number of events in the electron channel is smaller than the number in the muon channel. We expect lepton-jet correlations and parity asymmetries to be extremely small for fake leptons; for isolated leptons from heavy flavor, parity asymmetries are very small at tree-level, and small at higher-orders, while lepton-jet correlations might be a bit larger. Thus

$$\bar{F}^{QCD} > |F_+^{QCD}| > |F_-^{QCD}|,$$

even for isolated leptons. This leads us to expect

$$|F_{\pm}^{tbq}| \gg |F_{\pm}^{QCD}|.$$

except possibly for  $F_+$  in the muon channel. The dominant source for  $F_+$  will be from muons emitted at large angles during  $b\bar{b}$  and  $c\bar{c}$  events. The kinematics of these events can be studied using a double-tagged sample. We believe, therefore, that even if the contribution of QCD muon events to  $F_+$  is large enough to be a concern, its size and shape can be determined from the data.

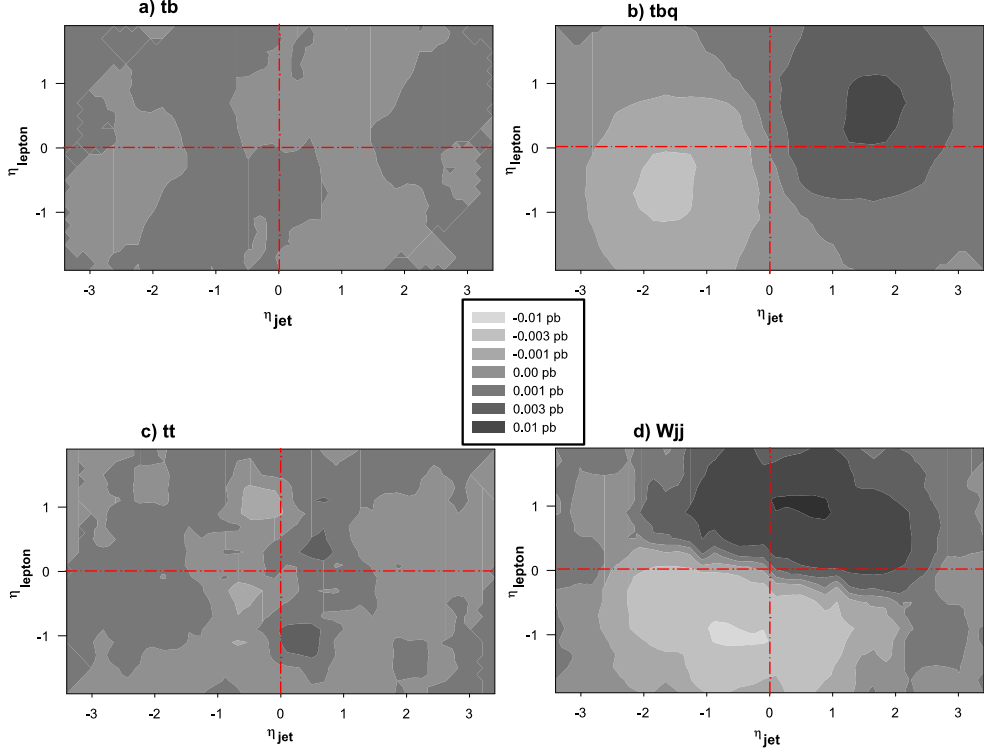


FIG. 7: Contour plots for the function  $F_-$  ( $\hat{\eta}_j, \hat{\eta}_\ell$ ) for a)  $tb$ , b)  $tbq$ , c)  $t\bar{t}$ , and d)  $Wjj$  channels (summed over  $t$  and  $\bar{t}$ ,  $e$  and  $\mu$ ).

### E. Lessons and Caveats

We can now extract some important lessons from Table VII. Before doing so, we should comment on its limitations.

First, our study is done entirely using tree-level short-distance matrix elements; only the normalizations are at next-to-leading order. We must therefore emphasize that *the figures and tables in this paper are meant for illustration only*. Next-to-leading-order corrections to the matrix elements will change the shapes of the background, in ways which contribute nontrivially to Table VII. For example, we expect the above-mentioned next-to-leading-order effects on  $t\bar{t}$  to affect our estimates of  $F_{\pm}^{t\bar{t}}$ , by something of order 10% of  $\bar{F}^{t\bar{t}}$ , which is not negligible. Such changes are large enough that they must be calculated and/or measured, but are small enough that they do not invalidate the *methodology* we are outlining here.

Second, it is clear from the table that statistical errors from the background are large in  $F_+$  and  $F_-$ , comparable to the signal. While this looks discouraging, it applies for the distributions integrated over the entire A or B quadrant. A quick examination of Fig. 3 shows that the situation is not quite as bad as it appears, if one considers the region away from the center of the  $(\hat{\eta}_j, \hat{\eta}_\ell)$  plane, where the backgrounds are much smaller and the signals are still quite large. We will discuss this in much more detail in the next section, where we will do a more sophisticated analysis, but for the moment we simply note that the size of the statistical errors is misleadingly large in the above table. Still, we will see that the situation with statistics remains unsatisfactory.

With these caveats in mind, we return to Table VII, on the basis of which we suggest the following general approach. One should first construct, for both the data and the Monte Carlo simulation output, the  $\bar{F}$ ,  $F_+$  and  $F_-$  functions. Using these functions, as well as information obtained from other measurements, one can systematically test one's understanding of each process. The  $\bar{F}$  function allows a measurement of the sum of the backgrounds without much contamination from signal. We assume that the separation of  $Wj^n$  from  $t\bar{t}$  can be obtained using the fact that the  $t\bar{t}$  process can be measured and predicted with reasonable accuracy, using other data samples and Monte Carlo simulation. One can then cross-check one's understanding of the shape of the  $Wj^n$  background using the part of the  $F_-$  distribution (located roughly in quadrant A) where the signal is negligible. Finally, one can attempt to measure

the signal from  $F_+$  and from a different part (located largely in quadrant B) of the  $F_-$  distribution.<sup>8</sup> Effects on  $F_+$  from QCD events with isolated leptons can be cross-checked by study of double-tagged events, and by comparing  $F_+$  for electrons against  $F_+$  for muons.

We now proceed to refine this approach, and to estimate the associated uncertainties.

#### IV. UNCERTAINTIES AND OPTIMIZATION

Our goal in this section is to show that the measurement of the signal using  $F_+$  and  $F_-$  is potentially feasible, though difficult. We begin this section with an overview that, using Figs. 8 and 9 as guides, lays out our main points. We then turn to more detailed consideration of statistical and systematic uncertainties, especially those associated with  $W$ -plus-jets.

##### A. Overview

Figure 8 shows the signal-to-background ratio for the differential cross-sections and for the three orthogonal functions that we have defined. Figure 8b shows the ratio

$$\frac{\bar{F}^{tbq} + \bar{F}^{tb}}{\bar{F}^{t\bar{t}} + \bar{F}^{Wjj}}$$

according to our simulations. Nowhere in the plane is the signal-to-background ratio of order unity, implying that sensitivity to even small systematic errors is severe. Instead,  $\bar{F}$  should be viewed as insensitive to the signal, and therefore mainly useful in helping determine of the size of the backgrounds.

Figures 8c and 8d show the analogous ratios

$$\left| \frac{F_+^{tbq} + F_+^{tb}}{F_+^{t\bar{t}} + F_+^{Wjj}} \right|$$

and

$$\left| \frac{F_-^{tbq} + F_-^{tb}}{F_-^{t\bar{t}} + F_-^{Wjj}} \right|$$

(We use absolute values for these two functions, as both numerator and denominator can be negative.) For both  $F_+$  and  $F_-$ , the signal-to-background ratio reaches unity in some parts of the plane, implying that, for sufficiently high statistics, *the signal can be measured in these two observables even if the background has relatively large systematic errors*. In both cases, the dark regions are the best ones for the measurement; the other regions should be cut away.

In Fig. 9 the ratio of signal to the square-root of background-plus-signal is plotted, for a integrated luminosity of 3 fb<sup>-1</sup>. Figure 9b shows

$$\frac{\bar{F}^{tbq} + \bar{F}^{tb}}{\frac{1}{2}(\bar{F}^{t\bar{t}} + \bar{F}^{Wjj} + \bar{F}^{tbq} + \bar{F}^{tb})^{1/2}}$$

while Figs. 9c and 9d show

$$\frac{|F_+^{tbq} + F_+^{tb}|}{\frac{1}{2}(\bar{F}^{t\bar{t}} + \bar{F}^{Wjj} + \bar{F}^{tbq} + \bar{F}^{tb})^{1/2}}$$

and

$$\frac{|F_-^{tbq} + F_-^{tb}|}{\frac{1}{\sqrt{2}}(\bar{F}^{t\bar{t}} + \bar{F}^{Wjj} + \bar{F}^{tbq} + \bar{F}^{tb} + F_+^{t\bar{t}} + F_+^{Wjj} + F_+^{tbq} + F_+^{tb})^{1/2}}$$

---

<sup>8</sup> Note that the study in [6] measures half this information; it is able to measure  $\bar{F}$  and the difference of quadrants  $A$  and  $B$  in  $F_-$ .



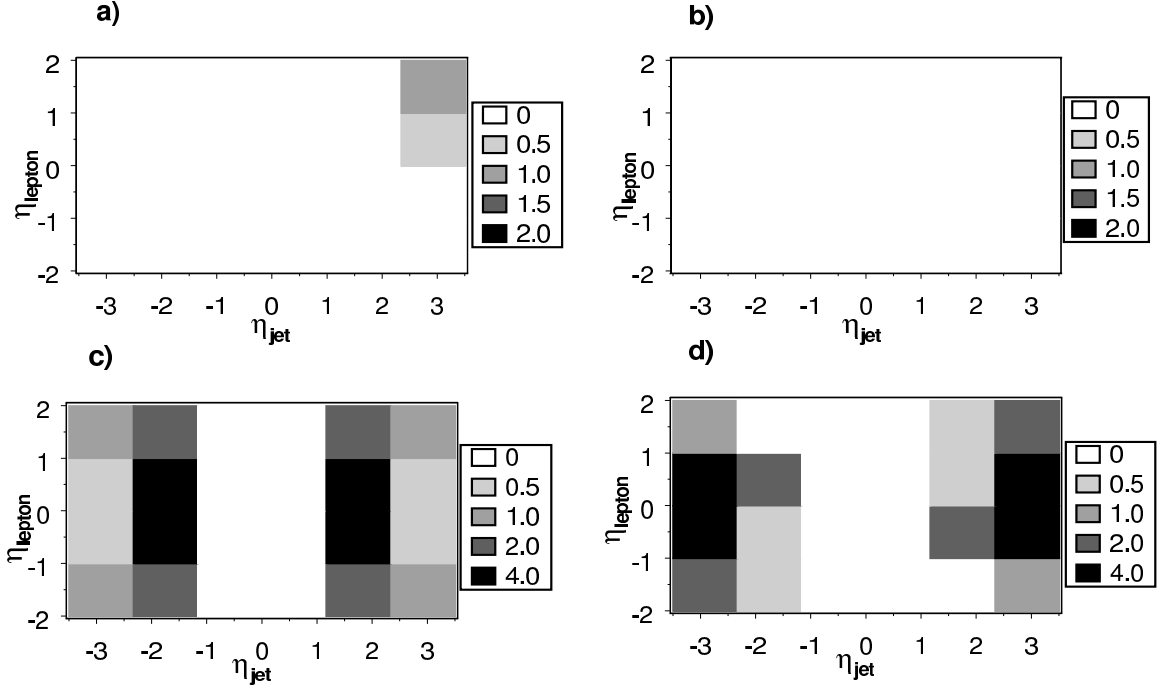


FIG. 8: Signal-to-background ratio  $S/B$  across the  $(\hat{\eta}_j, \hat{\eta}_\ell)$  plane, showing, within each  $1.16 \times 1.0$  bin in  $\hat{\eta}_j \times \hat{\eta}_\ell$ , the ratio of signal to background for a)  $\int d^2\sigma/d\hat{\eta}_j d\hat{\eta}_\ell$ , b)  $\bar{F}$ , c)  $|F_+|$  and d)  $|F_-|$ .

(Note that, by construction,  $\bar{F} > F_+$  for any distribution, so the expression under the square-root is always positive.) The form of the denominators (and the factors of  $1/2$  and  $1/\sqrt{2}$ ) follow from ordinary Gaussian statistics for each bin, using the definitions of  $\bar{F}$  and  $F_\pm$ , Eqs. (3)–(4), as linear combinations of statistically independent bins.<sup>9</sup> The possibility of aggregating bins into larger regions, in which these ratios are of order 1.2, is illustrated using the dot-dash outlined bins in the case of  $F_+$  and  $F_-$ .

Figures 8 and 9 show that *there is nonzero overlap, for both  $F_+$  and  $F_-$ , between the region where the statistics is best and the region where sensitivity to systematic errors is small.* Moreover, we learn that *the two measurements should use data predominantly from certain “windows” in the  $(\hat{\eta}_j, \hat{\eta}_\ell)$  plane.* The region where the jet has small  $|\hat{\eta}_j|$  has severe problems with statistical background and sensitivity to systematics. The  $F_+$  measurement should be made, roughly speaking, by using all data for  $\hat{\eta}_j > 1$  and any  $\hat{\eta}_\ell$ , (recall that the regions with either or both  $\hat{\eta}$  negative are redundant in the case of  $F_+$ .) Meanwhile the  $F_-$  measurement of the signal should be made, roughly, by cutting away all but the region  $\hat{\eta}_j > 1$  and  $\hat{\eta}_\ell > -1$  (the mirror-symmetric region  $\hat{\eta}_j < -1$  and  $\hat{\eta}_\ell < 1$  being redundant in this case.)<sup>10</sup>

<sup>9</sup> For instance,  $F_-$ , defined in Eq. (5), satisfies

$$\Delta F_- = \frac{1}{2} \left[ \left\{ \Delta \left( \frac{d^2\sigma}{d\hat{\eta}_j d\hat{\eta}_\ell}(\hat{\eta}_j, \hat{\eta}_\ell) \right) \right\}^2 + \left\{ \Delta \left( \frac{d^2\sigma}{d\hat{\eta}_j d\hat{\eta}_\ell}(-\hat{\eta}_j, -\hat{\eta}_\ell) \right) \right\}^2 \right]^{1/2}.$$

Since the two terms in the right-hand side are uncorrelated,

$$\Delta F_- = \frac{1}{2} \left[ \left( \frac{d^2\sigma}{d\hat{\eta}_j d\hat{\eta}_\ell}(\hat{\eta}_j, \hat{\eta}_\ell) \right) + \left( \frac{d^2\sigma}{d\hat{\eta}_j d\hat{\eta}_\ell}(-\hat{\eta}_j, -\hat{\eta}_\ell) \right) \right]^{1/2} = \frac{1}{\sqrt{2}} (\bar{F} + F_+)^{1/2},$$

where we used Eqs. (3) and (4). This explains the formula used in Fig. 9d.

<sup>10</sup> We do not mean to imply that we are specifying the precise form of these windows. Their shapes must be optimized for each particular

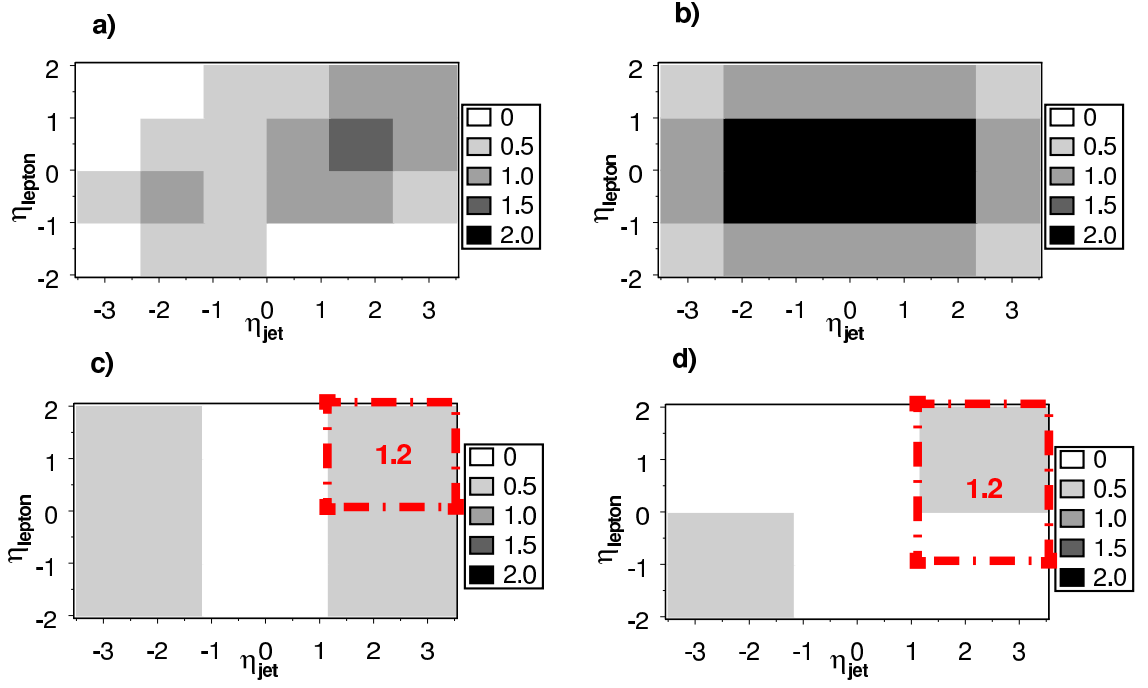


FIG. 9: Statistical significance  $S/\sqrt{B+S}$ , for an integrated luminosity of  $3 \text{ fb}^{-1}$ , across the  $(\hat{\eta}_j, \hat{\eta}_\ell)$  plane. Within each  $1.16 \times 1.0$  bin in  $\hat{\eta}_j \times \hat{\eta}_\ell$ , the number of events in a)  $\int d^2 \sigma / d\hat{\eta}_j d\hat{\eta}_\ell$ , b)  $\overline{F}$ , c)  $|F_+|$  and d)  $|F_-|$ , divided by the appropriate square-root of the number of events in background plus signal (see text for formulas.) For each box outlined in dot-dashed lines, the accompanying number indicates the improved value of  $S/\sqrt{B+S}$  that results when the bins inside the box are combined.

Let us also call attention to the region  $\hat{\eta}_j < 1$  and  $\hat{\eta}_\ell > 1$  for  $F_-$  (ignoring the redundant mirror-symmetric region), away from the center of the plane but also outside the above-mentioned  $F_-$  window. Here, the signal is very small. This region is useful for a check of the modeling of the  $Wj^n$  background. In the standard model, the contribution of  $F_-$  should be consistent with the  $Wj^n$  background, with little  $t\bar{t}$  and QCD background, and no measurable signal. Verifying that this is the case is both a cross-check on the analysis and a test of the standard model, so the measurement of  $F_-$  in this region is also very important.

## B. Statistical Errors

To explore the size of statistical errors, we have carried out two unsophisticated likelihood analyses, one optimistic, one overly pessimistic. In both cases, we assume  $3 \text{ fb}^{-1}$  of integrated luminosity. We assume that the shapes of the backgrounds and signals are known, and we fit for their normalizations. This is not quite appropriate, since some information about the normalization of the backgrounds will be known from other sources, and since there are significant uncertainties in the shape functions, especially for  $Wj^n$ , but we believe the measure we obtain is not far from the truth, and that the correct lesson can be extracted.

In the first likelihood analysis, somewhat optimistic, it is assumed that the shape of the distribution, in the  $(\hat{\eta}_j, \hat{\eta}_\ell)$  plane, of the sum of all backgrounds,  $t\bar{t}$  plus  $Wj^n$  (plus QCD) is known. Similarly, it is assumed that the shape of the

---

analysis, based on the associated backgrounds, acceptances, detector issues, and integrated luminosity, as well as improved simulations. Also, no window cut need actually be used; a fit or neural network will naturally weight the data inside the windows heavily, while down-weighting the regions outside the windows.

signal,  $tbq$  plus  $tb$ , is known. Maximizing the likelihood as a function of the relative normalization of the signal over background, we find that the measurement of signal over background can be made to a precision of about 40 percent.

For the second likelihood analysis, it is assumed that the shape of  $t\bar{t}$  (plus QCD) is known, the shape of  $Wj^n$  is separately known, and, as before, the shape of the signal  $tbq$  plus  $tb$  is known. We then fit for the two relative normalizations, and find that the measurement of the signal over the background can be made to a precision of about 50 percent. Meanwhile the measurement of the relative normalizations of the two backgrounds can be performed with an uncertainty of order 15 percent.

Both of these analyses show that statistical uncertainties are large even for  $\mathcal{L} = 3 \text{ fb}^{-1}$ , probably comparable to or larger than the theoretical uncertainties in the shapes of the distributions for the signals and backgrounds. To the extent that normalizations of the backgrounds can be pinned down using other information, the situation may be slightly better than this estimate suggests.

Intuitively, from the figures, the region in the center of the  $(\hat{\eta}_j, \hat{\eta}_\ell)$  plane plays a large role in fixing the backgrounds, while the large- $\hat{\eta}_j$  region of quadrant B plays a large role in fixing the signal. Indeed, as noted earlier, the statistical significance of the measurement in the signal comes dominantly from the regions outlined in dot-dashed lines in Fig. 9. Both measurements of  $F_+$  and  $F_-$  in these “windows” have  $S/\sqrt{B+S}$  of order 1.2, reasonably consistent with the above likelihood analyses, which were applied to the full distributions over the entire plane.

### C. Systematic Errors: General Comments

We now turn our focus to systematic uncertainties, which mainly stem from an inability to predict and simulate the backgrounds. Our use of the  $F_-$  and  $F_+$  functions, we will argue, helps us reduce the sensitivity of the measurement to systematic uncertainties. However, the systematic errors on the backgrounds are very large at present, and must still be reduced.

Earlier in this section, using Fig. 8, we discussed the signal-to-background ratios for the various component functions. We noted that Fig. 8b indicates that  $\bar{F}$  has a poor signal-to-background ratio. Although it has been argued that systematic uncertainties in predicting  $\bar{F}$ , using a combination of Monte Carlo simulations and data, will not be large, even a 15 percent systematic uncertainty is already enough to make  $\bar{F}$  problematic for measuring the signal, no matter how good the statistics. Instead, it is better to treat  $\bar{F}$  as a measurement which, along with other inputs, is used to help fix the normalizations of the backgrounds.<sup>11</sup>

Fig. 8c and 8d show that the situation with  $F_\pm$  is much better, outside of the central region of the plane where the background peaks.  $F_+$  may receive some additional contributions which we have neglected. There is a QCD contribution, which we have argued is probably small, especially in the electron channel. Detector effects and correlations from cuts can also contribute to  $F_+$ . This means the signal-to-background ratio in the figure may be an overestimate.<sup>12</sup>

Meanwhile,  $F_-$ , the P-odd C-odd observable, has the feature that many potential sources of systematic uncertainty largely cancel. We expect QCD backgrounds, correlations from cuts, and effects of detector cracks or damage to be small in this variable, since they are largely P-even and/or C-even. Many uncertainties in simulating  $t\bar{t}$  and even, to a degree,  $Wj^n$  will have substantial cancellations. This makes this variable especially compelling.

Eventually, the contribution of  $t\bar{t}$  to  $F_\pm$  should not have large systematic uncertainties. It is important to keep in mind that there are non-negligible effects, including a parity asymmetry [21], that appear at one loop. Next-to-leading-order calculations of the distributions in the  $(\hat{\eta}_j, \hat{\eta}_\ell)$  plane are needed. These can be computed with small errors and should allow a precise background subtraction of  $t\bar{t}$ . At present, however, their absence causes a substantial uncertainty in this subtraction.

For both  $F_+$  and  $F_-$ , the most serious systematic problems stem from the uncertainties in the shape of  $Wj^n$ . For this reason, we will now present an extended discussion of this background.

<sup>11</sup> In the counting experiment discussed in Sec. III.A, one essentially uses  $\bar{F}$  to make the measurement, though with much tighter cuts than the “relaxed cuts” employed here.

<sup>12</sup> Moreover, it appears in the figure to be somewhat better than we actually expect it to be, perhaps by as much as a factor of two in any given bin. In our simulations there is some accidental cancellation between the  $Wj^n$  and  $t\bar{t}$  contributions to  $F_+$ ; see Fig. 6. Unfortunately our knowledge of these two backgrounds is too poor to be certain that this cancellation is robust, and moreover statistical fluctuations may also ruin the cancellation.

$Wjj$ Channel	$\sigma(\text{before tags})$ [fb]	$\sigma(\text{after tags})$ [fb]	Fraction tagged
$Wqq$	16,470	192	1%
$Wqg$	32,000	732	2%
$Wgg$	14,760	484	3%
$Wcq$	3200	318	10%
$Wcg$	2240	238	11%
$Wc\bar{c}$	600	104	17%
$Wb\bar{b}$	496	224	45%
Total	69766	2291	3%

TABLE VIII: The cross sections for  $Wj^n$  events with at least two jets, before and after tagging of one of the jets. Each row refers to the combination of processes with the tree-level final state shown in the left-most column. The  $Wcq$  and  $Wcg$  entries include both  $c$  and  $\bar{c}$  quarks; the symbol  $q$  stands for  $u, d, s, \bar{u}, \bar{d}, \bar{s}$ . After showering, hadronization and jet identification, and application of the cuts in Table I, the resulting cross section is indicated in the next column. The cross section corresponding to a single tagged jet is shown in the third column, while the last column shows the ratio of the previous two. Simulation uncertainties in these numbers are of order  $\pm 1\text{--}3\%$ , except for the  $Wqg$  and  $Wqq$  channels, with uncertainties of order  $\pm 4\%$  and  $\pm 8\%$ , respectively. The (much larger) systematic uncertainties are discussed in the text.

#### D. Systematic Errors: Predicting $W$ -plus-jets

One might hope that systematic errors stemming from the  $Wj^n$  background could be greatly reduced, for the variables  $F_\pm$ , using a sideband subtraction in the variable “ $m_t$ ”. This approach, analogous to the method suggested in [1] for use in a counting experiment, would allow a background subtraction without much theoretical input. However, any such attempt will run into the same issues that cause this method to fail for a counting experiment. In Fig. 2, we showed that the application of aggressive cuts to bring  $Wj^n$  under statistical control simultaneously makes a sideband analysis problematic by deforming the shape of the  $Wj^n$  background, leaving it non-monotonic across the region needed for the sideband analysis. To do a subtraction therefore requires that the shape of the background, after cuts, to be accurately *predicted*, using a combination of theory, Monte Carlo and data. Unfortunately, prediction of any aspects of  $Wj^n$ , especially with one or more  $b$ -tagged jets, is very difficult indeed. As we will now discuss in detail, we believe that Monte Carlo results for the  $Wj^n$  sample with  $b$ -tags cannot currently be trusted at the level that is likely to be needed.

The shape of the  $Wj^n$  background is plagued with the usual concerns about the inability of Pythia or Herwig [22] to reliably generate the correct pattern of additional radiated jets; for recent discussion, see [23]. But to this and other typical problems, which are known to be issues in many processes, we must add some others which are specific to the sample with one (and only one)  $b$ -tagged jet. (Note the event samples used in our single-top analysis above include events with one *or more* tagged jets; however, the problems detailed in this section are somewhat less severe for samples with more than one tag.)

A striking feature of this sample is that only a moderate fraction of  $Wj^n$  events with a single tagged jet (and passing our cuts) actually have a short-distance  $b$ -quark parton present in the hard-scattering process; those that do are mainly  $Wb\bar{b}$ . Instead, the single  $b$ -tag sample is composed of many different contributions. This situation is made explicit in Table VIII, which shows the cross-section for various  $Wjj$  channels, before and after the requirement of a single tag, and Table IX, which lists the relative contributions from the various  $Wjj$  channels to the single tagged sample. As with all our simulations, these contributions were calculated using Madgraph [14] to evaluate the parton cross sections, Pythia [15] to provide showering and hadronization, and PGS [16] as the detector simulation of jet identification and tagging. The total  $Wj^n$  cross-section (before tagging) was normalized to the one-loop result [18]. The basic cuts of Table I were used; note that an untagged jet was also required in the event. The labels  $Wxy$  in the first column indicate the perturbative final state at tree-level (as evaluated in Madgraph); here  $q$  represents a light quark or antiquark ( $u, d, s, \bar{u}, \bar{d}, \bar{s}$ ). In Table VIII, the cross-section for each channel, before and after the requirement of a single tagged jet, is shown; also shown is the ratio of after-tagging to before-tagging (*i.e.*, the fraction of each channel containing a single tagged jet.) In Table IX, the three central columns divide the tagged events by whether the jet that was tagged in the event contained a bottom hadron, a charm hadron, or no heavy flavor. For example, the entry in the  $b$ -jet column of the  $Wqg$  row indicates that 11 percent of the entire  $Wj^n$  single-tag sample arises from  $Wqg$  events ( $q = u, d, s, \bar{u}, \bar{d}, \bar{s}$ ) in which the tagged jet contains bottom hadrons, mainly due to the splitting  $g \rightarrow b\bar{b}$  in the parton showering. In determining the entries in Table IX from those in Table VIII, we have attempted

$Wjj$ Channel	$b$ -jet	$c$ -jet	non- $b/c$ -jet	Total
$Wqq$	2%	1%	6%	9%
$Wqg$	11%	8%	14%	33%
$Wgg$	7%	5%	5%	17%
$Wcq$	0%	14%	1%	15%
$Wcg$	1%	10%	0%	11%
$Wc\bar{c}$	0%	5%	0%	5%
$Wb\bar{b}$	10%	0%	0%	10%
Total	31%	43%	26%	100%

TABLE IX: A budget of the sample of  $Wj^n$  events with a single tagged jet (and containing at least one untagged jet), constructed as in the previous table. Each entry shows the fraction of the sample containing a single-tagged jet that was generated from the tree-level process labelling the row (as in Table VIII) and in which the tagged jet was of the class labelling the column. The  $Wcq$  and  $Wcg$  entries include both  $c$  and  $\bar{c}$  quarks; the symbol  $q$  stands for  $u, d, s, \bar{u}, \bar{d}, \bar{s}$ . The entries in this table are subject to an additive uncertainty of  $\pm 1 - 2\%$ . The (much larger) systematic uncertainties are discussed in the text.

to correct for any double counting. For example, we have subtracted the contribution to the  $b$ -jet  $Wgg$  entry (from  $g \rightarrow b\bar{b}$  in the parton shower) arising from events with kinematic configurations already present in the  $b$ -jet  $Wb\bar{b}$  entry. This leads to small corrections, of order the stated  $\pm 2\%$  uncertainty, in several of the entries.

The central feature of these tables is the multitude of contributions to the tagged sample, all of similar magnitude. As clearly visible in Table VIII, the large parton-level cross-sections for the light quark and gluon processes are reduced by a low tagging fraction, while the much smaller tree-level heavy-quark cross-sections are subject to much larger tagging rates. Consequently, within the single-tag sample, all such partonic processes end up contributing at roughly at the same level, as is clear in the “after-tagging” column of Table VIII, and in the “total” column of Table IX. The breakdown of the resulting single-tag sample by the fraction of the sample for which the tagged jet is a bottom jet, a charm jet, or a jet without heavy flavor is visible in Table IX; as the numbers in the bottom row indicate, all contributions are again of the same order.

The simulations were performed with statistics sufficient to ensure such that each entry in Table IX is subject to an *additive* statistical uncertainty of order 2–3%. However, the systematic uncertainties in the simulations are much larger, due to a host of important physical and technical issues. Since these systematic uncertainties are the most important obstacle to an accurate background estimate, we now discuss them in detail.

Consider first the uncertainties in the basic event simulation. A precision simulation of the  $Wjj$  sample cannot, at present, be carried out. The parton-level theoretical computation of the differential cross-section for  $W$  plus two or more high  $p_T$  jets has been advanced in recent years:  $Wjj$  has been calculated to next-to-leading order, and  $Wjjj$  is known at leading-order. While the program “MCFM” [9, 18] can provide accurate next-to-leading-order parton-level cross-sections, no event generator valid at next-to-leading order currently exists. Consequently, there is at present no possibility of simulating this background without significant theoretical uncertainties.

Moreover, even when a next-to-leading-order event generator becomes available, there are serious questions concerning showering algorithms that must be addressed. The main problem is associated with the splitting of gluons to heavy quarks (or more precisely, with tuning Pythia or Herwig to simulate correctly the process in which a partonic gluon generates one or more jets containing charm or bottom mesons.) As illustrated in Table IX, a substantial fraction of the single-tagged sample, of order 33% in our simulations, originates from this process. It is not known with confidence how often gluons at short distance lead to jets with charm or bottom hadrons, or how often this process leads to two jets rather than one. Studies on this issue that compare data from LEP [24] and Tevtron [25] with QCD expectations [26] and with Pythia and Herwig suggest that there is no serious disagreement. However, this conclusion rests on the substantial uncertainties (of order 30%) in both the experimental and the theoretical results. Generally the perturbative predictions (including resummed logarithms) and the Monte Carlo results (with default parameters) tend to underestimate the observed rates of heavy flavor production in parton showers. Also, the rough agreement speaks mainly to overall rates of heavy-flavor production, not to charm-to-bottom ratios or kinematic distributions. Given the large sensitivity of the single-tag sample to these effects, it appears that a sizeable uncertainty in both the normalization and shape of the  $Wj^n$  background arises from this source.

A related issue is the role of uncertainties in parton distribution functions. The single tag sample receives significant contributions from events with charm in the final state that arise from initial states containing non-valence partons. Examples include processes such as  $u\bar{s} \rightarrow W^+u\bar{c}$ ,  $g\bar{d} \rightarrow W^+g\bar{c}$ , and  $\bar{u}\bar{d} \rightarrow W^+\bar{u}\bar{c}$ . These processes have varying shapes

and rates, and depend on the poorly-determined parton distribution functions.

Even if one could precisely simulate these events, there is still the issue of determining the efficiencies for tagging of jets with bottom or charm quarks, and for mistagging of jets with neither. This must be done as a function of  $p_T$  and pseudo-rapidity. As indicated in Table IX, each of these tagging processes plays a comparable role in determining the  $Wjj$  sample. Uncertainties in tagging functions thus lead to uncertainties in the shape of  $Wj^n$  which cannot be ignored. An especially serious issue is that the ratio of  $c$  to  $b$  tagging rates is currently extracted not from data but from Monte Carlo programs, which, among other problems, are dependent upon the correct modelling of gluons splitting to heavy flavor.

Clearly, it would be beneficial to decrease the mistagging and charm-tagging efficiencies *relative* to the efficiency for tagging of bottom jets. This would improve the ratio of the signal to the  $Wj^n$  background, reducing sensitivity to systematic errors, and also would directly suppress some of the main sources of uncertainty in the prediction of  $Wj^n$ . However, tuning the  $b$ -tagging algorithm to improve purity of the sample generally comes at the cost of a small reduction in the  $b$ -tagging efficiency, which in turn decreases the signal and increases statistical errors. The right balance between these competing issues is detector- and luminosity-dependent and must be left to the experimental collaborations.

Another related concern is the subtle linkage between  $b$ -tagging, jet definitions, and gluon splitting. When a gluon splits to two heavy quarks, the probabilities to obtain one tagged jet, two tagged jets, or one tagged and one untagged jet depend upon all three issues. This may mean that the separation of the samples with one tag versus two tags is unstable and not well predicted by theory. It is for this reason that we have chosen to consider samples with one-or-more tagged jets. Alternatively, one might require strong angular separation between tagged jets in order to retain predictivity.

A further issue involves the potentially large sensitivity of the shape and normalization of the multi-channel  $Wj^n$  background to the cuts used to bring backgrounds under control. In particular, both the  $H_T$  and  $m_t$  cuts used in the current analysis and in recent experimental papers [6] reshape the  $Wj^n$  background. While it has been shown [1] that jet vetoes are effective at substantially reducing the size of  $t\bar{t}$  backgrounds, we would argue against the use of this approach. The systematic errors which jet vetoes introduce into the prediction of the  $Wj^n$  background has not been quantified, but we expect it is prohibitively large. We are especially concerned about the requirement of two-and-only-two jets employed in [6]. We believe this will make the prediction of  $Wj^n$  unreliable, both because of problems with QCD corrections, and because of failures to correctly model the rate at which gluons in parton-level processes lead to zero, one or two jets containing heavy flavor. There is at present no consensus as to the safest method for reducing  $t\bar{t}$ , or, for that matter,  $Wj^n$ . We would like to argue strongly that this is a very important problem, which our methods simultaneously mitigate and highlight. On the one hand, neither the  $F_+$  nor the  $F_-$  distribution is strongly sensitive to the overall size of  $t\bar{t}$ . Consequently, the use of a strong jet veto or harsh  $H_T$  cut is unnecessary, and indeed unjustified to the extent systematic errors in  $Wj^n$  become larger as a result. Our approach would instead prefer a method which cuts  $t\bar{t}$  less severely, and in a safer fashion, such that theoretical errors in predicting  $Wj^n$  remain small. The  $H_T$  cut that we use is, we believe, safer, being a cut on a more inclusive variable; whereas the splitting of one jet into two, due to a fluctuation or a changed jet algorithm, affects a jet veto in a dangerous way, this is not so for an  $H_T$  cut. But this safety is only relative; there are problems with jets moving above or below the minimum  $p_T$  required for a jet to be included in the variable  $H_T$  that we defined. In any case, our method requires less focus on reducing the size of  $t\bar{t}$  and more focus on keeping  $Wj^n$  as small and as predictable as possible.

With all these problems in view, any method used to extract the  $Wj^n$  background will have to pass many cross-checks. One important consistency check can be carried out by calibrating Monte Carlo simulations using both  $Wj^n$  and the process  $Z$ -plus-jets (“ $Zj^n$ ”), where the  $Z$  decays leptonically. The processes  $Wj^n$  and  $Zj^n$  do not have the same shapes, rates, and heavy flavor content, so one cannot directly take ratios of distributions or even of overall cross-sections. However, the overall kinematics of  $Zj^n$  is similar to  $Wj^n$ , and is similarly sensitive to all of the above-mentioned issues. For these reasons, we expect that matching a Monte Carlo to the rates and shapes of the  $Zj^n$  and  $Wj^n$  distributions from data, with zero, one or two tagged jets, will significantly reduce systematic uncertainties. Such matching will require adjusting parameters which affect the splitting of gluons to heavy flavor, and adjusting tagging functions.<sup>13</sup> It would also be very helpful if direct measurements of the bottom-content, charm-content, and non- $b$ /non- $c$  content of the various single- and double-tagged  $Wj^n$  and  $Zj^n$  samples could be carried out, even with low precision and confidence. This would allow direct tests of numerous Monte Carlo predictions that at present have very large uncertainties. Studies of the  $Zb$  to  $Zj$  ratio have been carried out [27], but the challenging study of  $Zc$  separately should also be considered as statistics improve.

In summary, determining the single-tagged  $Wj^n$  cross-section will require a carefully crafted combination of theory,

---

<sup>13</sup> We believe there should be enough  $Z$ -plus-jets data, with  $3\text{ fb}^{-1}$  of integrated luminosity, for this analysis to be carried out.

data, and theory-optimized Monte Carlo.

## V. SUMMARY

A counting experiment for discovery of electroweak single-top production appears very challenging. In an effort to improve the situation, we have explored the possibility of using the distinctive shape of this process to separate it from background. We use as observables the pseudo-rapidity  $\eta_j$  of the leading- $p_T$  untagged jet and the pseudo-rapidity  $\eta_\ell$  of the charged lepton, weighted by the charge of the lepton  $Q_\ell$ . (One of these variables was already used in [4, 6].) Considering the distributions of signal and background in the  $(\hat{\eta}_j, \hat{\eta}_\ell)$  plane (where  $\hat{\eta}_j = Q_\ell \eta_j$  and  $\hat{\eta}_\ell = Q_\ell \eta_\ell$ ), we have noted that the distributions for  $t\bar{t}$  and for QCD are largely symmetric, while that of the signal is not; the  $Wj^n$  ( $W$ -plus-jets) background is intermediate between them. Constructing functions  $\bar{F}$ ,  $F_\pm$ , defined in Eqs. (3)-(5), which have various symmetry properties, we have shown that the statistical and systematic errors in the functions  $F_\pm$ , which are orthogonal to the function  $\bar{F}$  that would be used in a counting experiment, can be brought close to reasonable size without using extreme cuts.

Here is a summary of key ingredients that went into this analysis, as well as a list of elements which we did not account for, and a few of our crucial assumptions:

- All cross-sections ( $tb, tbq, t\bar{t}, Wbb, Wcc, Wcq, Wcg, Wqq, Wqg, Wgg$ ) were calculated at tree level.
- These were then normalized to theoretical calculations at next-to-leading order. For  $Wj^n$ , only the sum of all channels was normalized in this way.
- All processes were run through Pythia, to simulate showering, and through the detector simulation PGS.
- We imposed hard  $p_T$  cuts on the leading tagged and untagged jets, and required that a top quark be reconstructable from the lepton, tagged jet, and missing energy. We applied an  $H_T$  cut aimed at reducing  $t\bar{t}$ ; we did not use a jet veto.
- $p_T$ -dependence of tagging fractions was accounted for, with the maximal tagging rates at high  $p_T$  for  $b, c, q/g$  being taken as 50%, 15%, 1%. The details of the analysis are sensitive to these numbers, as well as to the rate for hard gluons at leading order to evolve into jets containing heavy flavor.
- We did not attempt to simulate QCD events. Instead, we argued QCD effects are (in theory) sufficiently symmetric in shape and (from DZero data) sufficiently small in rate that their contributions to all useful observables can be neglected (with the possible exception, for DZero, of  $F_+$  in the muon channel.)
- We discussed important shape effects on  $t\bar{t}$  at next-to-leading order [21], which we expect to be about ten percent or less, but did not simulate them.

It should be noted that we have not optimized our cuts to improve efficiencies and reduce systematics in a rigorous way. Indeed, it would not be too useful to do so, since the optimization is a moving target, depending on integrated luminosity, on tagging rates and other detector details, on next-to-leading-order shapes, and on Monte Carlo assumptions. We believe, therefore, that our results could be improved upon through such an optimization, though this is only worth doing in a concrete analysis. We also have not explored whether other methods of reconstructing  $m_t$  might be more effective, or whether variables other than  $H_T$  might be better as far as both statistics and systematics. This is certainly something that should be done as the integrated luminosity increases.

Moreover, there is a natural extension of our method which we did not consider, but which should be explored if the integrated luminosity becomes sufficiently high. Our observable  $F_+$  focussed on lepton-jet pseudo-rapidity correlations, but as we pointed out, these correlations can have two sources: *inherent* correlations in the rest frame of the  $tbq$  system (or of the top quark itself) and correlations which are *induced* by the boosting of these frames into the lab frame. Both of these effects are present in the signal, and they add coherently to give a large contribution to  $F_+$ . One could imagine measuring the two effects separately. This could potentially allow for even greater separation of signal from background.

We conclude with a summary of and comments upon what we see as the main lessons of our analysis.

1) Our method largely removes  $t\bar{t}$  and QCD events from the observables  $F_\pm$ , making extreme cuts on  $t\bar{t}$  unnecessary, and focussing attention on  $Wj^n$  as the main background. While the statistical fluctuations from  $t\bar{t}$  are still important, they are of less concern than systematic errors on  $Wj^n$ , since the former scale as the square-root of the  $t\bar{t}$  rate, while the latter scale linearly with the  $Wj^n$  rate. Moreover, the  $t\bar{t}$  background is much more safely calculated and simulated,

and will be, in the end, easier to remove. In our approach to single top, *one should not cut hard on  $t\bar{t}$  if doing so causes the systematic uncertainties in  $Wj^n$  to increase substantially.* In particular, this argues against the use of a severe jet veto, in which events with more than two observed jets are discarded.

2) The method that we have introduced requires that the shapes of  $t\bar{t}$  and  $Wj^n$  be properly modeled, but it also provides for cross-checks. The function  $\bar{F}$  measures the total background, and, assuming  $t\bar{t}$  can be determined using other samples, this allows a measurement of the total  $Wj^n$  background. Meanwhile, there is a region in the  $(\hat{\eta}_j, \hat{\eta}_\ell)$  plane where the  $F_-$  function gets small contributions from both signal and from  $t\bar{t}$ . This region allows a check of whether the shape of  $Wj^n$  has been correctly understood, as well as being interpretable as a worthwhile test of the standard model itself.

3) The thorniest problem obstructing the measurement of single top is understanding the shape of the  $Wj^n$  background. This is a large and irreducible background which must be subtracted from the signal, even in the context of the methods we proposed here. This subtraction could be done directly, using our cuts, but this requires some prediction of the shape in the  $(\hat{\eta}_j, \hat{\eta}_\ell)$  plane. Alternatively, a sideband analysis around the “ $m_t$ ” window cut could be applied to  $F_\pm$ , in appropriate pseudo-rapidity windows, but this too requires prediction of the effect of cuts on the distribution of  $Wj^n$  in “ $m_t$ ” and pseudo-rapidity.

While theory, Monte Carlo and data all can, and must, assist with these subtractions, many different types of uncertainties plague the sample with a single  $b$ -tag (and therefore the sample with one-or-more  $b$ -tags), making it unclear how to bring all the available resources together. We believe that a dedicated study, examining the rates, shapes, and flavor content (especially of bottom versus charm) of both  $Wj^n$  and  $Zj^n$ , with zero, one and two tagged jets, will be necessary. This will require a blend of multiple measurements, theoretically precise predictions, and careful tuning and cross-checking of Monte Carlo simulations. Since this issue affects many other measurements, including the Higgs search and numerous beyond-the-standard-model searches, we view this as a very high priority.

4) There are very few paths toward reducing the  $Wj^n$  background relative to the signal. One clear need is to decrease the mistagging rate and charm-tagging efficiency while maintaining or increasing the  $b$ -tagging efficiency; this would both improve signal-to-background and reduce some of the uncertainties that make it difficult to model the background. Another important step would be taken if the resolution in reconstructing the top quark mass from the  $b$ , lepton and missing energy could be improved. This would allow a narrowing of the  $m_t$  window cut, which would both reduce the size of the  $Wj^n$  background and reduce experimental and theoretical uncertainties in any sideband analysis. Beyond this, one would need to consider more radical ideas, such as finding methods which could, on average, differentiate bottom jets from charm jets, bottom jets from antibottom jets, and/or jets formed by short-distance heavy quarks from jets formed by gluons that have split into roughly-collinear heavy quark pairs.

In conclusion, our method for extracting single-top confirms that one can use the distinctive shape of the signal to reduce backgrounds more effectively than in a pure counting experiment. However, we also find that backgrounds are much worse than was once thought. Improvements in (mis)tagging rates and in the understanding thereof, careful modeling of  $W$ -plus-jets cross-checked against both theory and data, and more theoretically trustworthy techniques for cutting away backgrounds will all be necessary for a robust measurement of single top production. The single-tag  $W$ -plus-jets background, in particular, represents a challenge that the whole community must meet head-on.

### Acknowledgments

We thank our colleagues G. Watts, A. Garcia-Bellido, T. Gadfort, A. Haas, H. Lubatti, and T. Burnett for many useful conversations and direct assistance. We also thank K. Ellis, T. Junk, S. Mrenna, T. Stelzer, Z. Sullivan and E. Thomson for extended conversations and for their thoughtful comments and criticisms. This work was supported by U.S. Department of Energy grants DE-FG02-96ER40956 and DOE-FG02-95ER40893, and by an award from the Alfred P. Sloan Foundation.

- 
- [1] T. Stelzer, Z. Sullivan, and S. Willenbrock, Phys. Rev. D **58**, 094021 (1998) [arXiv:hep-ph/9807340].
  - [2] For other previous studies of single top quark production see S. S. Willenbrock and D. A. Dicus, Phys. Rev. D **34**, 155 (1986); C. P. Yuan, Phys. Rev. D **41**, 42 (1990); S. Cortese and R. Petronzio, Phys. Lett. B **253**, 494 (1991); R. K. Ellis and S. J. Parke, Phys. Rev. D **46**, 3785 (1992); D. O. Carlson and C. P. Yuan, Phys. Lett. B **306**, 386 (1993); T. Stelzer, S. Willenbrock, Phys. Lett. B **357**, 125 (1995) [arXiv:hep-ph/9505433]; “Future Electroweak Physics at the Fermilab



- Tevatron: Report of the tev\_2000 Study Group,” edited by D. Amidei and R. Brock, Report No. FERMILAB-Pub-96/082 (1996); A. P. Heinson, A. S. Belyaev and E. E. Boos, Phys. Rev. D **56**, 3114 (1997) [arXiv:hep-ph/9612424]; A. S. Belyaev, E. E. Boos and L. V. Dudko, Phys. Rev. D **59**, 075001 (1999) [arXiv:hep-ph/9806332].
- [3] T. Tait and C.-P. Yuan, Phys. Rev. D **63**, 014018 (2001) [arXiv:hep-ph/0007298].
  - [4] CDF Collaboration (D. Acosta et al.), Phys. Rev. D **69**, 052003 (2004); *ibid.* D **65**, 091102 (2002) [arXiv:hep-ex/0110067].
  - [5] D0 Collaboration (B. Abbot et al.), Phys. Rev. D **63**, 031101 (2001) [arXiv:hep-ex/0008024]; D0 Collaboration (V.M. Abazov et al.), Phys. Lett. B **517**, 282 (2001) [arXiv:hep-ex/0106059].
  - [6] CDF Collaboration, (D. Acosta et al.), arXiv:hep-ex/0410058 (submitted to Phys. Rev. Lett.).
  - [7] See “Search for single top production” at <http://www-d0.fnal.gov/Run2Physics/WWW/results/prelim/T0P/T09/T09.pdf>.
  - [8] B.W. Harris et al, Phys. Rev. D **66**, 054024 (2002) [arXiv:hep-ph/0207055].
  - [9] J. Campbell, R. K. Ellis and F. Tramontano, arXiv:hep-ph/0408158.
  - [10] Q.-H. Cao, R. Schwienhorst, C.-P. Yuan, arXiv:hep-ph/0409040; Q.-H. Cao, C.-P. Yuan, arXiv:hep-ph/0408180.
  - [11] D. Acosta *et al.* [CDF Collaboration], arXiv:hep-ex/0404036.
  - [12] J. Campbell and J. Huston, arXiv:hep-ph/0405276.
  - [13] S. Mrenna and P. Richardson, arXiv:hep-ph/0312274.
  - [14] F. Maltoni and T. Stelzer, “MadEvent: Automatic event generation with MadGraph,” JHEP **0302**, 027 (2003) [arXiv:hep-ph/0208156].
  - [15] T. Sjostrand, P. Eden, C. Friberg, L. Lonnblad, G. Miu, S. Mrenna and E. Norrbin, Comput. Phys. Commun. **135**, 238 (2001) [arXiv:hep-ph/0010017]. Version 6.217 was used in this analysis.
  - [16] J.S. Conway *et al.* in Proceedings of the Workshop on Physics at Run II-Supersymmetry/Higgs, Fermilab, 1998, p.39 [arXiv:hep-ph/0010338].
  - [17] M. Cacciari, *et al.*, JHEP **0404** 068 (2004) [arXiv:hep-ph/0303085].
  - [18] J. M. Campbell, R. K. Ellis, Phys. Rev. D **62**, 114012 (2000) [arXiv:hep-ph/0006304]; *ibid.* D **65**, 113007 (2002) [arXiv:hep-ph/0202176].
  - [19] See <http://www-cdf.fnal.gov/physics/new/top/public/btag/> for relevant graphs.
  - [20] See, for example, G. Mahlon, arXiv:hep-ph/0011349, arXiv:hep-ph/9811219; Gregory Mahlon and Stephen Parke, Phys. Lett. B **476**, 323 (2000) [arXiv:hep-ph/9912458]; Phys. Rev. D **55**, 7249 (1997) [arXiv:hep-ph/9611367].
  - [21] J. H. Kuhn and G. Rodrigo, Phys. Rev. D **59**, 054017 (1999) [arXiv:hep-ph/9807420]. See also M. Fischer, *et al.*, Phys. Rev. D **65**, 054036 (2002) [arXiv:hep-ph/0101322].
  - [22] HERWIG 6.5, G. Corcella, I.G. Knowles, G. Marchesini, S. Moretti, K. Odagiri, P. Richardson, M.H. Seymour and B.R. Webber, JHEP **0101** (2001) 010 [arXiv:hep-ph/0011363]; arXiv:hep-ph/0210213.
  - [23] Z. Sullivan, Phys. Rev. D **70**, 114012 (2004) [arXiv:hep-ph/0408049].
  - [24] A. Ballestrero *et al.*, arXiv:hep-ph/0006259. See also K. Abe *et al.* (The SLD Collaboration), Phys. Lett. B **507**, 61 (2001) [arXiv:hep-ex/0102002]; R. Barate *et al.* (The ALEPH Collaboration), Phys. Lett. B **434**, 437 (1998); P. Abreu *et al.* (The DELPHI Collaboration), Phys. Lett. B **401**, 163 (1997); G. Abbiendi *et al.* (The OPAL Collaboration), Eur.Phys.J. **C18**, 447 (2001) [arXiv:hep-ex/0010029].
  - [25] D. Acosta *et al.* (CDF Collaboration), Phys. Rev. D **69**, 072004 (2004) [arXiv:hep-ex/0311051].
  - [26] See, for example, M. H. Seymour, Nuc. Phys. **B436**, 163 (1995); D.J. Miller and M. H. Seymour, Phys. Lett. **B435**, 213 (1998) [arXiv:hep-ph/9805414]; M.L. Mangano and P. Nason, Phys. Lett. B **285**, 160 (1992); M.L. Mangano, Nuc. Phys. **B405**, 536 (1993).
  - [27] See “Measurement of the Cross Section Ratio of Z+b/Z+j” at <http://www-d0.fnal.gov/Run2Physics/WWW/results/HIGGS/higgs.htm>.